

*Citation for published version:*

Taylor, PR, Baker, RE & Yates, CA 2014, 'Deriving appropriate boundary conditions, and accelerating position-jump simulations, of diffusion using non-local jumping', *Physical Biology*, vol. 12, no. 1, 016006.  
<https://doi.org/10.1088/1478-3975/12/1/016006>

*DOI:*

[10.1088/1478-3975/12/1/016006](https://doi.org/10.1088/1478-3975/12/1/016006)

*Publication date:*

2014

*Document Version*

Peer reviewed version

[Link to publication](#)

## University of Bath

### Alternative formats

If you require this document in an alternative format, please contact:  
[openaccess@bath.ac.uk](mailto:openaccess@bath.ac.uk)

#### General rights

Copyright and moral rights for the publications made accessible in the public portal are retained by the authors and/or other copyright owners and it is a condition of accessing publications that users recognise and abide by the legal requirements associated with these rights.

#### Take down policy

If you believe that this document breaches copyright please contact us providing details, and we will remove access to the work immediately and investigate your claim.

# Deriving appropriate boundary conditions, and accelerating position-jump simulations, of diffusion using non-local jumping

P R Taylor, R E Baker and C A Yates

Wolfson Centre for Mathematical Biology, Mathematical Institute, University of Oxford, Andrew Wiles Building, Radcliffe Observatory Quarter, Woodstock Road, Oxford, OX2 6GG, UK

E-mail: `paul.taylor@maths.ox.ac.uk`

**Abstract.** In this paper we explore lattice-based position-jump models of diffusion, and the implications of introducing non-local jumping; particles can jump to a range of nearby boxes rather than only to their nearest neighbours. We begin by deriving conditions for equivalence with traditional local jumping models in the continuum limit. We then generalise a previously postulated implementation of the Robin boundary condition for a non-local process of arbitrary maximum jump length, and present a novel implementation of flux boundary conditions, again generalised for a non-local process of arbitrary maximum jump length. In both these cases we validate our results using stochastic simulation. We then proceed to consider two variations on the basic diffusion model: a hybrid local/non-local scheme suitable for models involving sharp concentration gradients, and the implementation of biased jumping. In all cases we show that non-local jumping can deliver substantial time savings for stochastic simulations.

*Keywords:* Lattice-based position-jump models, diffusion, stochastic simulation, stochastic boundary conditions, non-local position-jump.

Submitted to: *Phys. Biol.*

## 1. Introduction

Lattice-based position-jump (LBPJ) models are a valuable stochastic tool for modelling in biology; their intuitive structure and relative ease of implementation make them well suited for interdisciplinary research. There has been particular interest in their application to processes such as embryonic development, cancer metastasis and wound healing (see, for example, [1], [2] and [3]), although similar models have also been applied to areas such as animal dispersal [4]. Simultaneously, other researchers have worked on refining and extending the theoretical framework of LBPJ models, with developments including results for diffusion on unstructured meshes and irregular geometries [5, 6, 7]. Although LBPJ models are a relatively efficient technique for stochastic simulation, they can become computationally intensive when used to simulate the dynamics of large numbers of particles. In this paper we demonstrate that allowing particles to jump to non-nearest neighbour boxes can significantly speed up the simulation of such models.

At present most LBPJ models allow only purely local jumping, so that a particle can travel only to a nearest neighbour site (see, for example, [8]), while others introduce a transition matrix approach, whereby any particle can jump to any box with some set probability (for example, [9]). We consider here an intermediate approach, where particles can make jumps of non-local but limited range. This approach can be used to speed up simulations of motile particles since fewer events need to be simulated. The first part of this paper is concerned with determining the conditions for mathematical equivalence between the standard, local jump process and our non-local jump process. In section 2 we provide a brief outline of LBPJ models and propose a general form for a non-local process of maximum jump length  $Q$ , which we expect to provide equivalent results to a local process in the mean-field limit.

Some LBPJ models may be considered to be equivalent to a partial differential equation (PDE) in the appropriate continuum limit, making possible a variety of comparative and hybrid models for multiscale problems. The importance of correctly applied boundary conditions for PDE problems is well known, but the problem of

implementing equivalent conditions in LBPJ models has received surprisingly little attention. This is despite work showing that the analytically correct implementations of simple PDE boundary conditions within a discrete model can be far from intuitive, and vary considerably depending on the form of the model [10]. In the second part of this paper, we begin by generalising an implementation of the Robin boundary condition to a non-local system (section 3), and note how this limits admissible values for the lattice spacing and/or the diffusion coefficient. In section 4 we present an implementation of flux boundary conditions in a LBPJ model, and show that for a non-local process of maximum jump length  $Q$ , terms representing flux over the boundary should directly affect the dynamics of the first  $Q$  boxes from the boundary, not just the closest one. We derive a generalised form for this boundary condition from the continuum limit.

Numerical investigations suggest that the behaviour of non-local systems can diverge from the behaviour of the equivalent local systems around sharp gradients in particle numbers. In section 5 we therefore consider how we can implement a hybrid approach, where regions without sharp gradients in particle concentrations can be modelled using non-local jumping while other regions use entirely local jumping. In section 6 we discuss how biased jumping for modelling asymmetric random walks can be implemented within our framework, and how this affects the boundary conditions. Finally, we conclude with a discussion of our results, and suggest avenues for further work that have been opened up by the results we present in this paper.

## 2. Non-local jumping for diffusion

We begin by defining a spatial lattice over the domain  $x \in [0, L]$  composed of  $K$  boxes of width  $h = L/K$ , as shown in figure 1, such that the centre of the  $i^{th}$  box will be located at  $x_i = (2i - 1)h/2$ . The distribution of particles over this domain is given by the vector  $\mathbf{m}(t) = [m_1(t), m_2(t), \dots, m_K(t)]$ , where  $m_i(t)$  denotes the number of particles in the  $i^{th}$  box at time  $t$ .

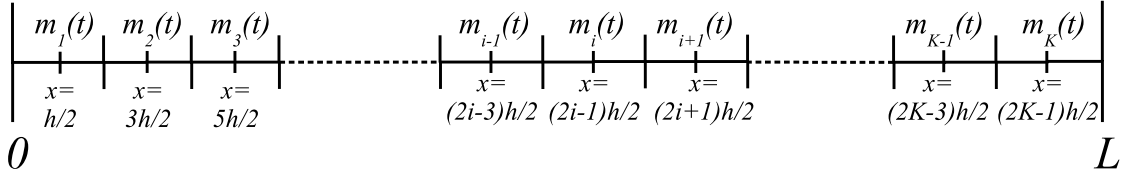


**Figure 1.** A representation of the spatial lattice for the individual-based stochastic model.

### 2.1. Local position-jump models

For  $2 < i < K - 1$ , particles in box  $i$  are permitted to jump to boxes  $i - 1$  or  $i + 1$ , with rates per unit time of  $T_i^-$  and  $T_i^+$ , respectively.

The mean number of particles in box  $i$  evolves according to

$$\frac{dm_i}{dt} = T_{i-1}^+ m_{i-1}(t) - (T_i^+ + T_i^-) m_i(t) + T_{i+1}^- m_{i+1}(t), \quad (1)$$

where  $\mathbf{m}(t) = [m_1(t), m_2(t), \dots, m_K(t)]$  is a vector of the mean number of particles at the lattice points. We now introduce a continuous function  $u(x, t)$  as a continuum approximation to these discrete values. There are several factors which might cause the jump rates to vary spatially, such as density of particles or the presence of some signalling profile. Several LBPJ models incorporating these features are described and implemented in [11] and [12]. In other models movement is restricted by permitting at most one particle to occupy each lattice site (see, for a recent example, [13]). For now, however, we will assume that jump rates are independent of both time and position, and that any number of particles may share the same position, so we drop the subscripts and write simply  $T^+$  and  $T^-$ . The right-hand side of (1) can be expanded using Taylor series about  $x$ , leading to

$$\frac{\partial u(x, t)}{\partial t} = h \frac{\partial u(x, t)}{\partial x} (T^- - T^+) + \frac{h^2}{2} \frac{\partial^2 u(x, t)}{\partial x^2} (x, t) (T^- + T^+) + o(h^2). \quad (2)$$

Note that in the unbiased case, where  $T = T^- = T^+$ , the first order terms cancel (we discuss biased jumping in section 6). Defining  $\lim_{h \rightarrow 0} Th^2 = D$  we recover the diffusion equation,

$$\frac{\partial u}{\partial t} = D \frac{\partial^2 u}{\partial x^2}. \quad (3)$$

## 2.2. Non-local jumping

For a non-local jump process, we write the rates of a jump  $q$  box-lengths to the left or to the right from position  $i$  as  $T_i^{-q}$  or  $T_i^{+q}$ , respectively. Jumps for which  $q = 1$ , i.e. jumps to adjacent boxes, are written  $T_i^{\pm 1}$  to distinguish them from  $T_i^{\pm}$ , the rates for the locally jumping process. For a system of maximum jump length  $Q$ , away from any boundary, assuming position independence again (i.e.  $T_i^{\pm q} = T^{\pm q}$ ), upon Taylor expanding about  $x$  we have

$$\frac{\partial u(x, t)}{\partial t} = -h \frac{\partial u}{\partial x}(x, t) \left( \sum_{q=-Q, q \neq 0}^Q q T^q \right) + \frac{h^2}{2} \frac{\partial^2 u}{\partial x^2}(x, t) \left( \sum_{q=-Q, q \neq 0}^Q q^2 T^q \right) + o(h^2). \quad (4)$$

Note again, that in the unbiased case, where  $T^{+q} = T^{-q} = T^q$ , the first order terms cancel. We compare the second order term to that of (2) and obtain the equivalence condition

$$T = \sum_{q=1}^Q q^2 T^q. \quad (5)$$

For example, for a non-local jumping process with  $Q = 2$ , this condition is

$$T = T^1 + 4T^2. \quad (6)$$

Clearly there are an infinite number of rate choices which satisfy this relationship, but we will specify the basic non-local jumping rate as

$$T^q = \frac{T}{Qq^2}, \quad (7)$$

where  $T$  is the jumping rate from the equivalent, local process. This satisfies (5) above, and also preserves the well-known relation that the mean squared displacement,  $\langle x^2 \rangle$ , of a particle scales linearly with time in a diffusion process. For example, doubling the jump distance reduces the rate at which jumps will occur by a factor of four. With this result we conclude the first part of this paper, and turn our attention to boundary conditions.

### 2.3. Example

To illustrate the accuracy of non-local jumping, and its potential to save computational time, we compare 1,000 local simulations to 1,000 non-local simulations where  $Q = 5$ . The domain  $x \in [0, 5]$  was divided into 50 boxes of width  $h = 0.1$ . We imposed periodic boundary conditions, and set  $D = 1$ , initializing 1,800 particles in a peak centred around  $x = 2.5$ , so that our initial condition is

$$m_i(0) = \begin{cases} (i - 17) * 25, & \text{for } 18 \leq i \leq 25, \\ 200 - ((i - 26) * 25), & \text{for } 26 \leq i \leq 33, \\ 0, & \text{otherwise,} \end{cases} \quad (8)$$

as shown in figure 2(a). Each repeat of the non-local simulation ran in an average of 11.7 seconds, compared to an average of 39.1 seconds for each repeat of the local simulation. Inspection of the averaged states of the non-local and local simulations at  $t = 1$ , and comparison to the solution of the diffusion equation  $u_t = Du_{xx}$ , in figure 2(c) shows the quality of the fit. We quantify this fit in figure 2(b) using the Histogram Distance Error (HDE) metric, which is given by

$$\text{HDE} = \frac{1}{2} \sum_{k=1}^K |n_k - p_k|, \quad (9)$$

where  $n_k$  is the number of particles in box  $k$  normalised against the total number of particles in the system, and  $p_k$  is the total number of particles predicted at  $x = x_k$  by the PDE solution, normalised against the area under the curve of that solution [14]. Our stochastic simulations, here and throughout the rest of the paper, were run using Gillespie's direct method for exact stochastic simulation [15]. To reduce the computational time required we incorporated some recycling of random numbers [16], and only updated propensity functions when necessary [17]. Averaged simulation results were compared to the solution of the diffusive limit PDE, generated using Matlab's `pdepe` function and a spatial mesh of 8,001 points.

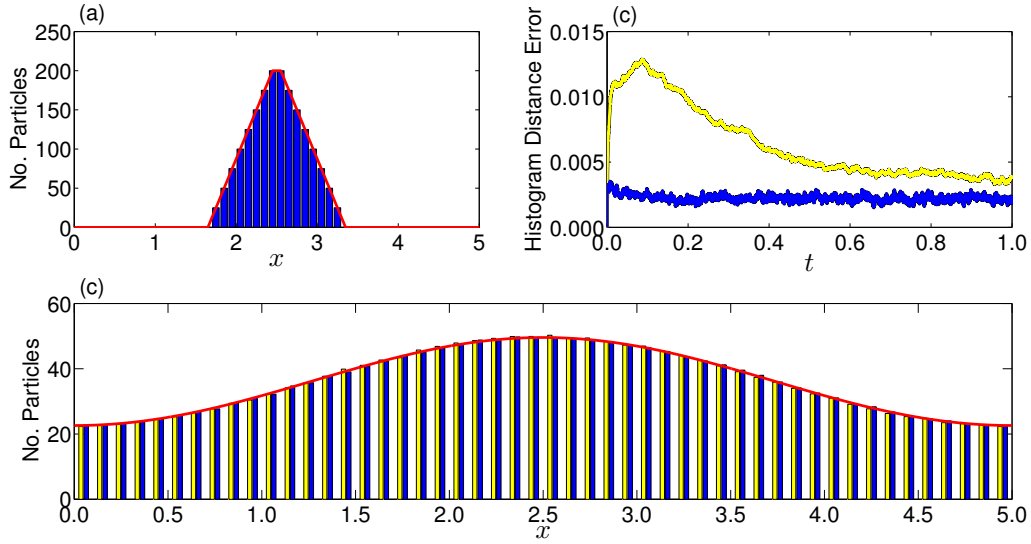


**Figure 2.** Average results from 2,000 repeats of a diffusion simulation from  $t = 0$  to  $t = 1$ , with periodic boundary conditions, as described in section 2.3. At time  $t = 0$ , we initialized 1,800 particles in a peak centred on  $x = 2.5$  (a). Half of the simulations were run using local jumping, and half using non-local jumping with  $Q = 5$ . In panel (c), it can be seen that the averaged state of the non-local simulations at  $t = 1$  (yellow bars) matches well to both the averaged state of the local simulations (blue bars) and the PDE solution (red line). The accuracy is confirmed by a HDE comparison of the local and non-local simulations to the solution of the limiting PDE (b).

### 3. The Robin boundary condition for local jumping

The first-order reactive boundary condition for the diffusion equation at  $x = 0$  is given by the Robin boundary condition,

$$D \frac{\partial u}{\partial x}(0, t) = Ru(0, t), \quad (10)$$

where  $R = 0$  describes a completely reflective boundary condition,  $R = \infty$  a completely absorbing one, and intermediate values describe different degrees of reactivity. The jump probability during some small time  $\Delta t$  is set to be  $D\Delta t/h^2$  for the local case. The reactive boundary condition at the left-hand boundary is implemented by declaring that any particle at  $x_1(t) = h/2$  which attempts to jump left is either reflected back to  $h/2$  with probability  $1 - P_{1,1}h$  or removed from the system with probability  $P_{1,1}h$  (we write



all adsorption probabilities in the form  $P_{q,Q}h$ , where  $q$  is the length of the jump and  $Q$  the maximum jump length of the system). It has been shown that the Robin boundary condition (10) is satisfied in the diffusive limit when  $P_{1,1} = R/D$  as follows [10]. The mean number of particles in the first box at time  $t + \Delta t$  is given by

$$m_1(t + \Delta t) = \left(1 - \frac{2D\Delta t}{h^2}\right) m_1(t) + \frac{D\Delta t}{h^2} \left[ m_2(t) + (1 - P_{1,1}h)m_1(t) \right]. \quad (11)$$

After rearranging, and multiplying through by  $\sqrt{\Delta t}$ , this becomes

$$\sqrt{\Delta t} \left( \frac{m_1(t + \Delta t) - m_1(t)}{\Delta t} \right) = \frac{D\sqrt{\Delta t}}{h} \left( \frac{m_2(t) - m_1(t)}{h} - P_{1,1}m_1(t) \right). \quad (12)$$

Taking the diffusive limit (i.e.  $\Delta t \rightarrow 0$ ,  $h \rightarrow 0$  such that  $\sqrt{\Delta t}/h$  remains constant), the left-hand side vanishes, and we arrive at

$$D \left. \frac{\partial u}{\partial x} \right|_{x=0} = DP_{1,1}u(0, t). \quad (13)$$

Comparison with (10) gives

$$P_{1,1} = R/D. \quad (14)$$

Although this argument is phrased in terms of discrete time steps, it is also applicable to continuous time simulations with small but non-zero box size  $h$  [10].

### 3.1. Extending to the $Q = 2$ case

Using the formula stated in (7) to relate the diffusion constant  $D$  to the transition rates, in the case where  $Q = 2$ , we find that  $D/2$  describes the rate of jumping to a neighbouring lattice site, and  $D/8$  the rate of jumping two lattice sites. In this section, and for the rest of this paper, we discuss implementing boundary conditions at the left-hand boundary without loss of generality.

We require two adsorption terms,  $P_{1,2}$  for when a molecule hits the boundary as a result of a length-one jump, and  $P_{2,2}$  for when the contact results from a length-two jump. Furthermore, we consider that the actual boundary is located at  $x = 0$ ,  $h/2$  left of  $x_1$ . In the local case, particles moving left from  $x_1$  will move  $h/2$  left before hitting the boundary and being reflected back  $h/2$  to the right, finishing at  $x_1$  where they began.

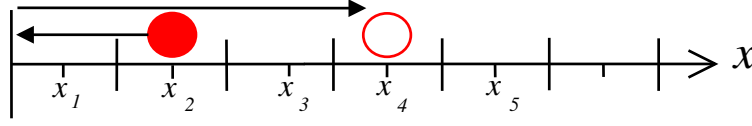


**Figure 3.** A particle (solid red circle) at  $x_2$  attempts to make a length-five jump leftwards. After moving  $3h/2$  to the left it hits the boundary and is reflected, travelling the remaining  $7h/2$  to the right to finish in  $x_4$  (empty red circle).

Analogously, in the non-local case, reflection therefore requires the particle to move leftwards as far as  $x_1$ , then making a further move of total length  $h$  to the boundary and back. If this is less than the total length of the jump, all remaining movement takes place in the rightwards direction, as shown in figure 3. So a leftwards length-two jump left from box 1 will end up in box 2, and a length-two jump from box 2 will end up in box 1 (assuming neither is adsorbed at the boundary). Then the equation for mean particle numbers at  $x_1$  is given by

$$m_1(t + \Delta t) = \left(1 - \frac{2D\Delta t}{2h^2} - \frac{2D\Delta t}{8h^2}\right) m_1(t) + \frac{D\Delta t}{2h^2} (m_2(t) + (1 - P_{1,2}h)m_1(t)) + \frac{D\Delta t}{8h^2} (m_3(t) + (1 - P_{2,2}h)m_2(t)), \quad (15)$$

which can be rearranged to give

$$\frac{m_1(t + \Delta t) - m_1(t)}{\Delta t} = \frac{D}{h^2} \left[ \left( \frac{-3 - 2P_{1,2}h}{4} \right) m_1(t) + \left( \frac{5 - P_{2,2}h}{8} \right) m_2(t) + \frac{1}{8} m_3(t) \right]. \quad (16)$$

We then multiply through by  $\sqrt{\Delta t}$ , and rearrange the terms to arrive at

$$\begin{aligned} \sqrt{\Delta t} \left( \frac{m_1(t + \Delta t) - m_1(t)}{\Delta t} \right) = D \left[ \frac{\sqrt{\Delta t}}{8} \left( \frac{m_1(t) - 2m_2(t) + m_3(t)}{h^2} \right) \right. \\ \left. - \frac{\sqrt{\Delta t}P_{2,2}}{8} \left( \frac{m_2(t) - m_1(t)}{h} \right) \right. \\ \left. + \frac{7\sqrt{\Delta t}}{8h} \left( \frac{m_2(t) - m_1(t)}{h} \right) + \frac{\sqrt{\Delta t}}{8h} (-P_{2,2} - 4P_{1,2}) m_1(t) \right]. \quad (17) \end{aligned}$$

We now take the limit as  $\Delta t, h \rightarrow 0$  while keeping the ratio  $\sqrt{\Delta t}/h$  constant. All the terms of (17) apart from the adsorption terms have been arranged into discretizations of exact derivatives, so the left-hand side, and the first two lines of the right-hand side

vanish due to the presence of  $\sqrt{\Delta t}$  terms. The remaining terms from the final line give

$$7D \left. \frac{\partial u}{\partial x} \right|_{x=0} = D(4P_{1,2} + P_{2,2})u(0, t). \quad (18)$$

Recalling the definition of the Robin boundary condition from (10), this reduces to

$$4P_{1,2} + P_{2,2} = \frac{7R}{D}. \quad (19)$$

Clearly this is not sufficient to specify  $P_{1,2}$  and  $P_{2,2}$  uniquely, so we examine the dynamics at  $m_2(t)$ :

$$\begin{aligned} m_2(t + \Delta t) &= \left( \frac{D\Delta t}{2h^2} + (1 - P_{2,2}h) \frac{D\Delta t}{8h^2} \right) m_1(t) + \left( 1 - \frac{2D\Delta t}{2h^2} - \frac{2D\Delta t}{8h^2} \right) m_2(t) \\ &\quad + \frac{D\Delta t}{2h^2} m_3(t) + \frac{D\Delta t}{8h^2} m_4(t). \end{aligned} \quad (20)$$

Simplifying, we find

$$\begin{aligned} \frac{m_2(t + \Delta t) - m_2(t)}{\Delta t} &= \frac{D}{8h^2} [(5 - P_{2,2}h)m_1(t) - 10m_2(t) + 4m_3(t) + m_4(t)] \\ &= \frac{D}{8} \left( \frac{m_2(t) - 2m_3(t) + m_4(t)}{h^2} \right) + \frac{6D}{8} \left( \frac{m_1(t) - 2m_2(t) + m_3(t)}{h^2} \right) \\ &\quad - \frac{P_{2,2}D}{8h} m_1(t) + \frac{D}{8h} \left( \frac{m_2(t) - m_1(t)}{h} \right). \end{aligned} \quad (21)$$

Again, upon multiplying by  $\sqrt{\Delta t}$  and taking the diffusive limit as before, the left-hand side and the first line of the right-hand side go to zero. The remaining terms give

$$D \left. \frac{\partial u(x, t)}{\partial x} \right|_{x=0} = P_{2,2} Du(0, t), \quad (22)$$

which, recalling the Robin boundary condition (10), gives us the adsorption rate for length-two jumps,

$$P_{2,2} = \frac{R}{D}. \quad (23)$$

Substituting this into the relationship derived by considering the dynamics in  $m_1(t)$ , (19), the adsorption rate for length-one jumps must be

$$P_{1,2} = \frac{3R}{2D}. \quad (24)$$

Since  $P_{1,2}h$  is a probability, it must be between zero and one in value, and we therefore note that this result imposes the constraint

$$0 \leq h \frac{R}{D} \leq \frac{2}{3}. \quad (25)$$

Hence for a given lattice and diffusion rate our choice of  $R$  is restricted, or conversely if a value of  $R$  has been specified then our choice of box size,  $h$ , will have to be sufficiently small. A similar constraint is observed in the local jumping implementation, but the condition becomes more restrictive in the non-local case as  $Q$  increases. We note that it is also possible to derive a non-local implementation of Robin boundary conditions in which the adsorption rates depend on the position that the reflecting particle is jumping from, rather than the length of the jump that took it to the boundary. In this  $Q = 2$  case, we would then have to require that particles jumping from the first box be adsorbed with probability  $Rh/D$ , and particles from the second box with probability  $3Rh/D$ . Since the larger of these probabilities here is greater than in the length-dependent case, it places a greater constraint on allowable values of  $R$ ,  $D$  and  $h$ . We therefore proceed by assuming that adsorption probabilities depend on the distance a particle is travelling, and not on its box of origin.

### 3.2. Generalised adsorption rates for any value of $Q$

The method used in the  $Q = 2$  case (i.e. rearranging terms into second derivatives which will vanish in the diffusive limit until only terms for  $x_1$  and  $x_2$  remain) can be used to derive a general result for any jump process of maximum jump length  $Q$ . At box  $k$ , where  $k \leq Q$ , the dynamics will be described by

$$\begin{aligned} \sqrt{\Delta t} \frac{dm_k}{dt} = & \frac{D\sqrt{\Delta t}}{Qh^2} \left[ \sum_{j=1}^Q \left( \frac{\chi_{[0,k-1]}(j)}{(k-j)^2} m_j(t) \right) + \sum_{j=1}^Q \left( \frac{1}{j^2} m_{k+j}(t) \right) \right. \\ & - \sum_{j=1}^Q \left[ \frac{\chi_{[0,k-1]}(j)}{(k-j)^2} + \frac{1}{j^2} \right] m_k(t) - \sum_{j=1}^{Q-k+1} \left[ \frac{1}{(j+k-1)^2} \right] m_k(t) \\ & \left. + \sum_{j=1}^{Q-k+1} \left[ \frac{1 - P_{j+k-1, Q} h}{(j+k-1)^2} m_j(t) \right] \right], \end{aligned} \quad (26)$$

where  $\chi_{[0,k-1]}(j)$  is an indicator function, equal to unity if  $0 \leq j \leq k-1$ , and zero otherwise. The two terms on the first line of the right-hand side represent particles jumping into the box at  $x_k$  from the left and right, respectively. The second line represents particles jumping from  $x_k$ , with the first set of brackets encompassing those

particles which jump without being reflected, and the second those which jump and are reflected. The final line represents those particles which are reflected into the box at  $x_k$ , having avoided being adsorbed by the boundary. We assume that the lattice is sufficiently large so that no influence from the boundary conditions at the right-hand boundary need be considered, i.e.  $K \geq 2Q$ .

The left-hand side of (26) will vanish in the diffusive limit, so we can focus on the right-hand side, rearranging it to the form,

$$\begin{aligned}
 0 = & \frac{D\sqrt{\Delta t}}{Qh^2} \left\{ \sum_{j=1}^{Q-k+1} \left[ \frac{1}{(j+k-1)^2} m_j(t) \right] - \left[ \sum_{j=1}^{Q-k+1} \frac{1}{(j+k-1)^2} \right] m_k(t) \right. \\
 & + \sum_{j=1}^Q \left( \frac{1}{j^2} m_{k+j}(t) \right) + \left( \sum_{j=1}^{k-1} \frac{1}{(k-j)^2} m_j(t) \right) - \left( \sum_{j=1}^{k-1} \frac{1}{(k-j)^2} + \sum_{j=1}^Q \frac{1}{j^2} \right) m_k(t) \\
 & \left. - \sum_{j=1}^{Q-k+1} \left[ \frac{P_{j+k-1,Q} h}{(j+k-1)^2} m_j(t) \right] \right\}. \tag{27}
 \end{aligned}$$

We have grouped the reflecting terms, non-reflecting terms, and adsorption events on separate lines. These three groupings are analysed separately in Appendices A, B and C, respectively. It can be shown that equation (26) can ultimately be rearranged, in the diffusive limit, to

$$0 = \frac{D}{Q} \left\{ \left( \sum_{j=k}^Q \frac{j-2k+1}{j^2} \right) \frac{\partial u}{\partial x} \Big|_{x=0} + \left( \sum_{j=k}^Q \frac{1}{j} \right) \frac{\partial u}{\partial x} \Big|_{x=0} - \sum_{j=k}^Q \left[ \frac{P_{j,Q}}{j^2} \right] u(0, t) \right\}, \tag{28}$$

plus a collection of terms which vanish in the limit. Rearranging again we obtain

$$D \sum_{j=k}^Q \left[ \frac{P_{j,Q}}{j^2} \right] u(0, t) = D \left( \sum_{j=k}^Q \frac{2j-2k+1}{j^2} \right) \frac{\partial u}{\partial x} \Big|_{x=0}. \tag{29}$$

Recalling that we wish to replicate the Robin boundary condition (10), this gives us an expression determining the adsorption rates:

$$\sum_{j=k}^Q \left[ \frac{P_{j,Q}}{j^2} \right] = \frac{R}{D} \sum_{j=k}^Q \left[ \frac{2j-2k+1}{j^2} \right]. \tag{30}$$

We see that  $P_{Q,Q} = R/D$  for any  $Q$ . For any other adsorption rate,  $P_{k,Q}$  ( $k \neq Q$ ), we note that the left-hand side of (30) can be written

$$\frac{P_{k,Q}}{k^2} + \sum_{j=k+1}^Q \left[ \frac{P_{j,Q}}{j^2} \right], \tag{31}$$

while the right-hand side can be written

$$\frac{R}{D} \left( \sum_{j=k+1}^Q \left[ \frac{2j-2k-1}{j^2} \right] + \sum_{j=k+1}^Q \left[ \frac{2}{j^2} \right] + \frac{1}{k^2} \right). \quad (32)$$

Since  $k < Q$ , and (30) holds for  $1 \leq k \leq Q$ , we can substitute  $k$  for  $k+1$  to obtain

$$\sum_{j=k+1}^Q \left[ \frac{P_{j,Q}}{j^2} \right] = \frac{R}{D} \sum_{j=k+1}^Q \left[ \frac{2j-2k-1}{j^2} \right], \quad (33)$$

so these terms cancel from (31) and (32). Substituting  $q$  for  $k$  and multiplying through by  $q^2$  we obtain our final result for  $q < Q$ :

$$P_{q,Q} = \frac{R}{D} \left( 1 + q^2 \sum_{j=q+1}^Q \left[ \frac{2}{j^2} \right] \right). \quad (34)$$

### 3.3. Example

To confirm these analytic results we ran 1,000 simulations, with a Robin boundary condition ( $R = 1$ ) at the left boundary, and a zero-flux boundary condition at the right boundary, comparing a local jump process to a non-local one with maximum jump length  $Q = 5$ . At time  $t = 0$  we set there to be 1800 particles in a peak centred on  $x = 1$ , as shown in figure 4(a), so that we have

$$m_i(0) = \begin{cases} (i-2) * 25, & \text{for } 3 \leq i \leq 10, \\ 200 - ((i-11) * 25), & \text{for } 11 \leq i \leq 18, \\ 0, & \text{otherwise.} \end{cases} \quad (35)$$

As can be seen in figure 4(c), the two match well, both with each other and to the solution of the diffusion equation with  $D = 1$ , i.e.  $u_t = u_{xx}$ . We quantify this fit in figure 4(b) using the HDE; the good agreement demonstrated by the HDE confirms the approximation to the diffusive limit. Furthermore, the non-local simulations each took 7.9 seconds to run on average, while the local simulations required on average 26.7 seconds each. We also study the convergence of the non-local implementation as  $h \rightarrow 0$ , by solving the appropriate master equations with the Euler method for decreasing values of  $h$ . We compare these results to the solution of the limiting PDE, and plot the HDE in figure 4(d), showing the convergence of the solution as  $h$  becomes smaller. The

PDE here, and in all other convergence studies in this paper, was solved using Matlab's PDEPE . For this example, we also plot the time taken to simulate this system for a range of particle numbers and lattice spacing, and it can be seen in figure 5 that non-local jumping provides the same relative acceleration for a range of lattice spacings and particle numbers in this case. This makes intuitive sense, as non-local jumping reduces computational time by effectively reducing the total jump rate of each individual particle, and so is not dependent on these other factors.

#### 4. Flux boundary conditions

It is possible to extend this work to derive flux boundary conditions (which correspond to inhomogenous Neumann boundary conditions when jumping is unbiased). Suppose, for example, we wish to enforce the boundary condition,

$$\left. \frac{\partial u}{\partial x} \right|_{x=0} = A. \quad (36)$$

We will treat  $A$  as a constant without loss of generality. Let us begin by considering only the case of positive flux into the system, i.e.  $A < 0$ .

##### 4.1. Flux conditions for local jumping

In the local case we need to add a term to the master equation for box one to account for particle influx. We require the number of new particles entering the system between times  $t$  and  $t + \Delta t$  to be proportional to  $\Delta t$ . Furthermore, we want the relative contribution of flux to the system to be independent of the choice of lattice size, so our term should be inversely proportional to the box size  $h$ . We will therefore write the contribution of the flux to the master equation as  $B_{1,1}\Delta t/h$  for some constant  $B_{1,1}$ , where the subscripted numbers indicate the box in question and the maximum jump length of the system, respectively.

Starting with the purely local jumping process, and treating the boundary as completely reflecting to jumping particles (hence providing zero net flux), the master

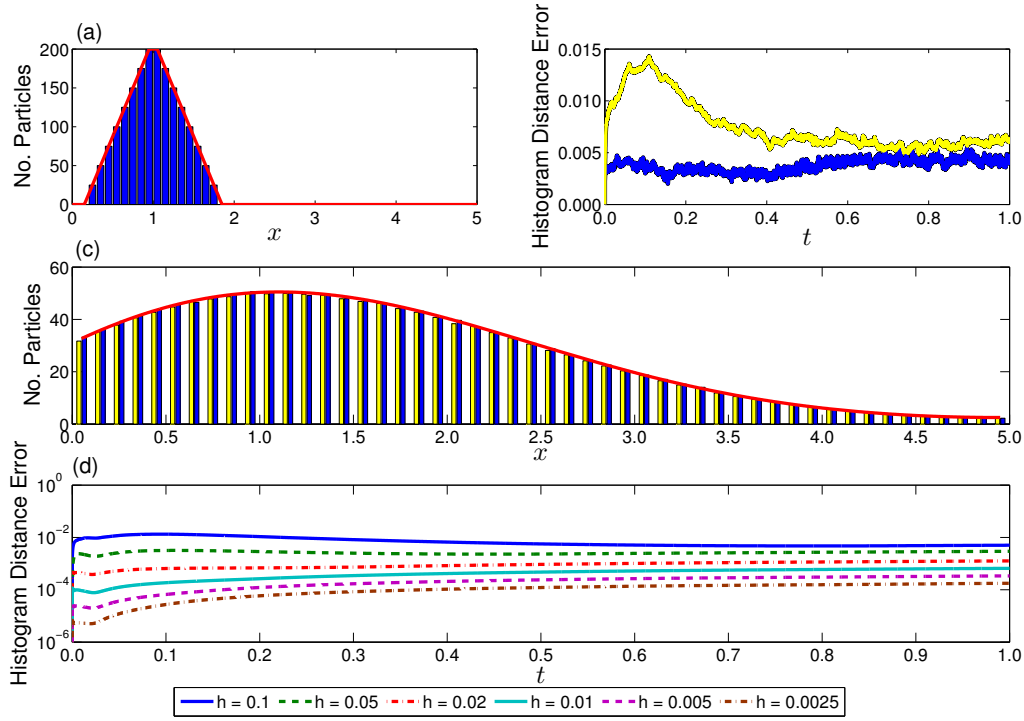


**Figure 4.** Averaged results from 1000 diffusion simulations (500 using local jumping, and 500 using non-local jumping) from  $t = 0$  to  $t = 1$ , with a zero-flux boundary condition at  $x = 5$  and a Robin boundary condition with  $R = 1$  at  $x = 0$ , as described in section 3.3. For our initial condition (a), we initialized 1,800 particles in the system in a peak centred around  $x = 1$ . The accuracy of the non-local boundary conditions is confirmed in (b) by a HDE comparison to the solution of the limiting PDE. This is also illustrated in panel (c), where we demonstrate that both the non-local ( $Q = 5$ , yellow bars) and local (blue bars) provide a good match to the PDE solution at  $t = 1$  when averaged over 500 iterations. As  $h$  becomes smaller, we see the solution of the master equations describing the non-local system with Robin boundary condition becomes closer to the solution of the limiting PDE (d).

equation for box 1 is

$$m_1(t + \Delta t) = \left(1 - \frac{D\Delta t}{h^2}\right) m_1(t) + \frac{D\Delta t}{h^2} m_2(t) + \frac{B_{1,1}\Delta t}{h}, \quad (37)$$

$$\Rightarrow \sqrt{\Delta t} \left( \frac{m_1(t + \Delta t) - m_1(t)}{\Delta t} \right) = \frac{\sqrt{\Delta t}}{h} \left( D \frac{m_2(t) - m_1(t)}{h} + B_{1,1} \right). \quad (38)$$

Taking the limit  $\Delta t \rightarrow 0$ ,  $h \rightarrow 0$  such that  $\sqrt{\Delta t}/h$  remains constant, this becomes

$$\left. \frac{\partial u(t)}{\partial x} \right|_{x=0} = -\frac{B_{1,1}}{D}. \quad (39)$$



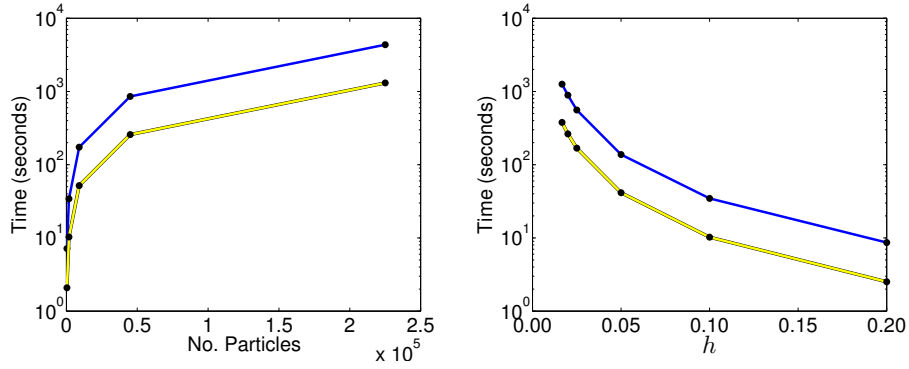


**Figure 5.** The time taken to run the simulation described in section 3.3 is seen in the left-hand figure to scale linearly with the number of particles in the system, while in the right-hand figure we see simulation time increasing nonlinearly as the box size  $h$  decreases (since the number of jumps in the system scales with  $1/h^2$ ). When varying particle numbers, we followed the relative distribution described in (35) while multiplying by a constant factor. When varying the lattice size, a fixed number of particles were split between the increased number of boxes. In both cases we see that the relative acceleration provided by non-local jumping is maintained for a range of particle numbers and lattice sizes.

Hence  $A = -B_{1,1}/D$ , and we can implement the Neumann boundary condition given by (36) by adding particles to box 1 at rate  $-AD/h$ . Figure 6 gives an example of this, confirming the accuracy of this implementation, starting from an initial distribution of

$$m_i(0) = \begin{cases} 105 - (10 * i), & \text{for } i \leq 10, \\ 0, & \text{otherwise,} \end{cases} \quad (40)$$

as shown in figure 6(a). We set  $D = 1$  as before, and impose boundary conditions

$$\left. \frac{\partial u(t)}{\partial x} \right|_{x=0} = -100, \quad (41)$$

$$\left. \frac{\partial u(t)}{\partial x} \right|_{x=5} = 0. \quad (42)$$

We note the good match between the local jumping simulation and the PDE at time  $t = 1$ , and the low value of the HDE, as shown in figures 6(c) and (b), respectively.

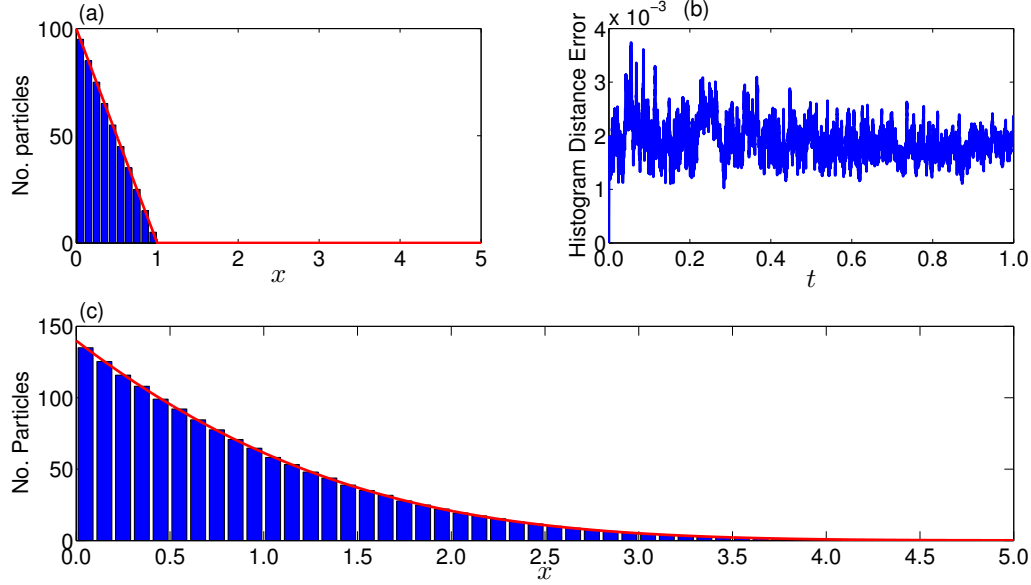


**Figure 6.** Average results from 1,000 repeats of a diffusion simulation from  $t = 0$  to  $t = 1$ , with a zero-flux boundary condition at  $x = 5$  and an in-flux boundary condition with  $A = -100$  at  $x = 0$ , as described in section 4.1. At time  $t = 0$ , we initialize 550 particles in the first ten boxes of the system following a linearly decreasing distribution (a). In panel (c), it can be seen that the local simulation (blue bars) matches well to the PDE solution (red line). The accuracy is confirmed by a HDE comparison to the solution of the limiting PDE (b).

#### 4.2. Generalised flux boundary conditions for non-local jumps

For a system in which non-local jumps of maximum length  $Q$  are allowed, particles must be added, not simply to the first box, but to the first  $Q$  boxes, with various weights. These weights should preserve the total flux into the system, and the general result for their distribution is given below. We parametrised the input with  $B_{1,1}\Delta t/h$  in the local case, so we will write the input term for the  $k^{th}$  box as  $B_{k,Q}\Delta t/h$ , in the non-local case.

The mean particle dynamics at  $x_k$  will be given by

$$\begin{aligned} \sqrt{\Delta t} \frac{dm_k}{dt} = & \frac{D\sqrt{\Delta t}}{Qh^2} \left\{ \left( \sum_{j=1}^Q \frac{\chi_{[0,k-1]}(j)}{(k-j)^2} m_j(t) \right) + \sum_{j=1}^Q \left( \frac{1}{j^2} m_{k+j}(t) \right) \right. \\ & \left. - \left( \sum_{j=1}^Q \frac{\chi_{[0,k-1]}(j)}{(k-j)^2} + \sum_{j=1}^Q \frac{1}{j^2} \right) m_k(t) - \left[ \sum_{j=1}^{Q-k+1} \frac{1}{(j+k-1)^2} \right] m_k(t) \right\} \end{aligned}$$

$$+ \sum_{j=1}^{Q-k+1} \left[ \frac{1}{(j+k-1)^2} m_j(t) \right] \Bigg\} + \frac{B_{k,Q} \sqrt{\Delta t}}{h}, \quad (43)$$

where  $1 < k \leq Q$ . We recognise this as the equation from the generalised Robin boundary case, but without adsorption and with an added input term  $B_{k,Q} \sqrt{\Delta t}/h$ . We can therefore reuse the results from Appendices A and B, and see that in the diffusive limit this equation will become

$$B_{k,Q} = -\frac{D}{Q} \left( \sum_{j=k}^Q \frac{j-2k+1}{j^2} + \sum_{j=k}^Q \frac{1}{j} \right) \frac{\partial u}{\partial x} \Big|_{x=0}. \quad (44)$$

Consolidating, and imposing the Neumann boundary condition again, this gives us the general formula for the input term at  $x_k$  in the reflecting case:

$$B_{k,Q} = -\frac{AD}{Q} \left( \sum_{j=k}^Q \frac{2j-2k+1}{j^2} \right). \quad (45)$$

By summing over  $1 \leq k \leq Q$  we obtain  $-AD$ , showing that the non-local boundary conditions conserve the total flux from the local boundary conditions.

#### 4.3. Example

In order to demonstrate the necessity of the derived non-local boundary conditions, rather than applying the simpler, local boundary condition where all new particles are added to the first box, we ran 1000 simulations of a non-locally jumping system with  $Q = 5$ , using the initial condition and boundary conditions used in the local jumping simulation in section 4.1, i.e. a no-flux boundary condition at  $x = 5$ , a Neumann condition with  $A = -100$  at  $x = 0$ , and the initial distribution of particles illustrated by figure 7(a). Each simulation was run from  $t = 0$  until  $t = 1$ , with  $D = 1$ . In half of these simulations we added new particles to the first five boxes, with rates as required by our result (45) with  $Q = 5$ . The other half of these simulations were identical, except that all new particles were added to the first box instead of being distributed over the first five. Figure 7(b) shows the superior fit of the data to the PDE limit in the first case, figure 7(c) shows the final state of the system, with a close-up of the first five boxes and illustrates how attempting to use the local implementation of a flux boundary

condition rather than the derived non-local implementation leads to deviation from the PDE solution. Each repeat of the non-local simulation ran in an average of 6.7 seconds, compared to 21.9 seconds for the equivalent local simulations shown in figure 6. As  $h$  becomes smaller, the non-local description can be seen in figure 7 to converge to the solution of the PDE.

## 5. Hybrid diffusion schemes

Our non-local jumping method gives results that match well with the results of the local jumping method in most cases but, in the case of sharp transitions in particle numbers, we have observed innaccurate results. We speculate that these result from our derivation of non-local jump rates in section 2.2, where the rates were chosen so that the second order terms in the expansion matched those of the expanded local model, but may result in fourth order and higher terms which differ from those of the local system and lead to different truncation errors [18]. In this light, it would therefore be useful if we could use non-local jumping in some regions of space to reduce the running time, but use local jumping in regions where the concentration changes rapidly in space so as to maintain accuracy.

We have already introduced an implementation of flux boundary conditions in non-locally jumping systems, and can therefore argue as follows. The lattice can be separated into two regions, with non-local jumping on the left domain and local on the right (again, without loss of generality). We can use the local jump rates to calculate the particle flux from left-to-right, and also from right-to-left, based on the number of particles in the boxes to either side of the boundary. For left-to-right movement, we implement a constant flux boundary condition using our result (45). Particles in the boxes concerned will otherwise continue to jump as normal, with any jump which would have taken them over the boundary reflecting instead: only the flux terms can take particles over the boundary to the right, and then only to the first local box. This means that additional, special jump rates for rightwards movement are required for particles in the  $Q$  boxes

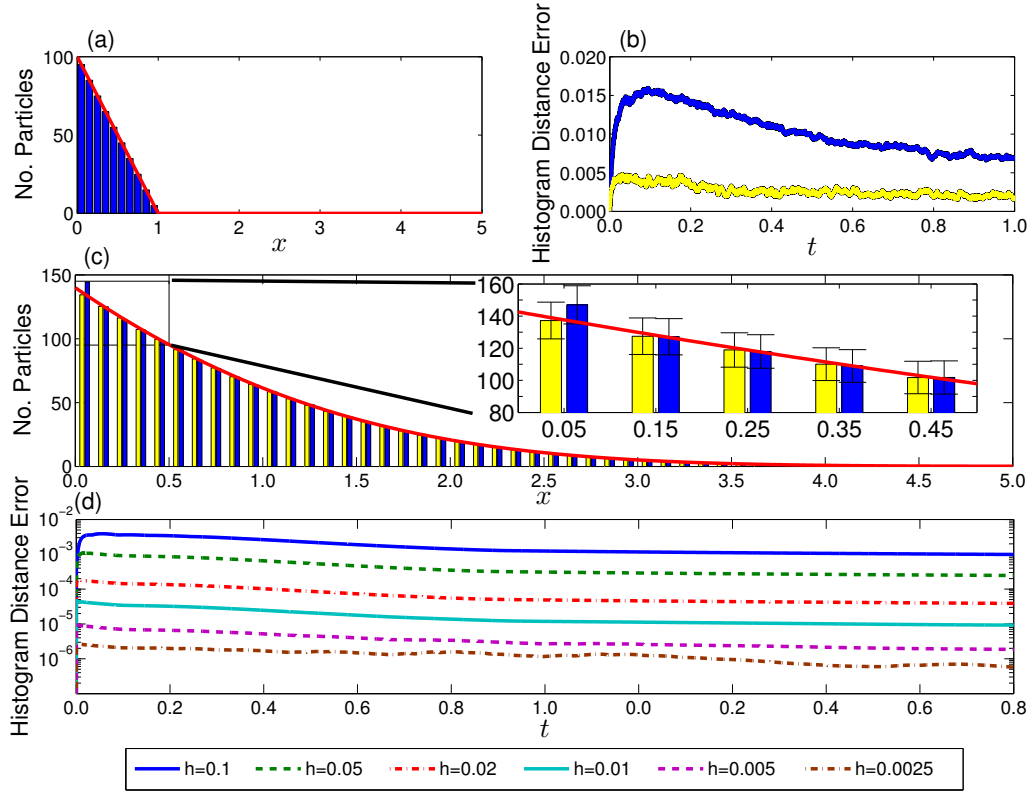


**Figure 7.** Average results from 1,000 repeats of a diffusion simulation from  $t = 0$  to  $t = 1$ , with a zero-flux boundary condition at  $x = 5$  and an in-flux boundary condition with  $A = -100$  at  $x = 0$ , as described in section 4.3. At time  $t = 0$ , we initialize 550 particles in the first ten boxes of the system following a linearly decreasing distribution (a). In panel (c), it can be seen that the non-local simulation with  $Q = 5$  and corresponding non-local boundary conditions (yellow bars) matches well to the PDE solution (red line), while the non-local simulation with local boundary conditions (i.e. all new particles added to the first box, shown by blue bars) deviates from this solution. The error is particularly evident in the first five boxes, as illustrated by the close-up (the error bars show the standard deviation of the results). This difference in accuracy is confirmed by a HDE comparison of both implementations to the solution of the limiting PDE (b), where the non-local simulation with the derived non-local boundary conditions is shown in yellow and the non-local simulation with local boundary conditions is shown in blue again. The apparent decline in the HDE for both implementations is an artifact of increasing particle numbers. In panel (d), we see the solution of the master equations describing the non-local system with flux boundary conditions becomes closer to the solution of the limiting PDE as  $h$  becomes smaller.

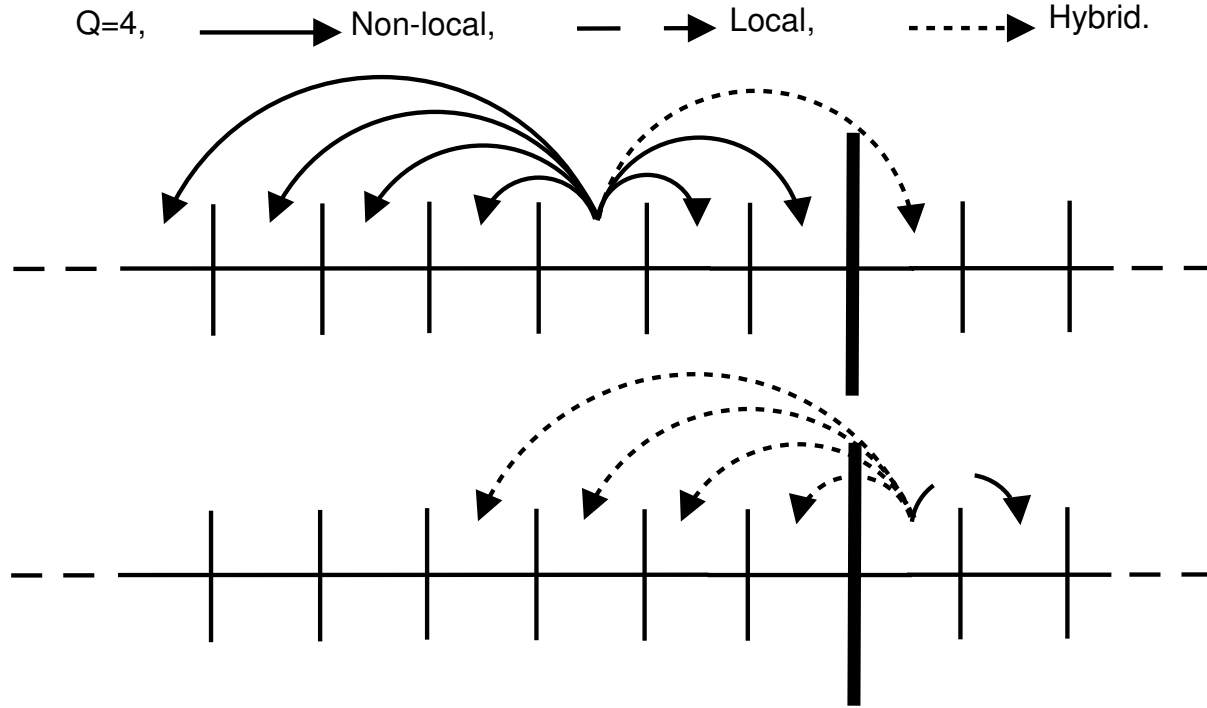


**Figure 8.** Example showing jumping options from boxes within the hybrid zone around the barrier for  $Q = 4$ . The non-local jumps denoted by solid lines all use standard non-local rates for their length; the dotted hybrid lines use Neumann based jumping rates. Reflecting particles are not shown.

closest to the boundary (all continue to jump left with unchanged rates).

We now consider movement from right-to-left. Since the right domain is locally jumping, we only have to implement special conditions in the first box. Particles in this box may jump right as normal, or jump left with the same probability. When jumping left, however, they may travel up to  $Q$  sites, with probabilities chosen to match the rates with which particles in those boxes are moving to the right. By implementing the boundary in this way, we maintain expected levels of flux between the two regions.

An implementation on these conditions for  $Q = 4$  is illustrated in figure 8.

### 5.1. Method

We define  $B_{k,Q}$ , the rate with which a particle from a box  $k \leq Q$  places to the left of the boundary will cross the boundary into the first box of the local domain, as

$$B_{k,Q} = -\frac{A_n D}{Q} \left( \sum_{j=k}^Q \frac{2j - 2k + 1}{j^2} \right), \quad (46)$$

where  $A_n D$  is a measure of the expected flux over the boundary to the right, and is given by multiplying the number of particles in the cell closest to the boundary on the non-local side by the local jumping rate. Conversely, particles in the first local box to the right of the boundary can jump up to  $Q$  places to the left, with rates given by

$$B'_{k,Q} = -\frac{A_l D}{Q} \left( \sum_{j=k}^Q \frac{2j - 2k + 1}{j^2} \right), \quad (47)$$

where  $A_l D$  is the multiple of the number of particles in the cell closest to the boundary on the local side and the local jumping rate (i.e. the expected jump rate over the boundary from right to left).

### 5.2. Example

We consider a simple morphogen gradient system, where particles are generated in boxes in the left-half of the domain with probability  $5000\Delta t$ , and decay with probability  $100\Delta t$ . In the diffusive limit this corresponds to the PDE

$$\frac{\partial u}{\partial t} = \frac{\partial^2 u}{\partial x^2} + 5000H(2.5 - x) - 100u, \quad (48)$$

where  $H(x)$  is the Heaviside function. Starting from an empty lattice at time  $t = 0$ , we ran 1,000 simulations until time  $t = 1$  of a standard non-local implementation, and another 1,000 of a hybrid non-local model with the interface between domains at  $x = 1.5$ . The maximum jump length was  $Q = 5$  in both cases. The results are shown in figure 9. Figure 9(a) shows the averaged final state of the system, with the hybrid model (yellow bars) matching the PDE solution (red line) closely, while the unmodified non-local process deviates slightly around the concentration gradient. The hybrid simulations each took on average 31.4 seconds to run, compared to 43.4 seconds for an equivalent

local simulation (not shown), but clearly more significant time saving would be made for simulations with larger morphogen production regions, or higher equilibrium particle numbers in that region. Sharp spatial gradients can also be accomodated by using a finer grid size, and figure 9(d) shows how the master equations representing the non-local system converge to the solution of the PDE as  $h$  becomes smaller.

## 6. Boundary conditions for biased diffusion

To incorporate biased diffusion, we divide our probabilities of movement into a symmetric diffusion term, which can be treated non-locally as usual, and an advection term promoting movement in the favoured direction. The probability of jumping in either direction over time step  $\Delta t$  as a result of diffusion is still given by  $D\Delta t/h^2$  as usual, while the additional probability of jumping in the favoured direction is given by  $b\Delta t/h$ , for some constant  $b$ . It can be shown that this will produce the advection-diffusion equation in the diffusive limit,

$$\frac{\partial u}{\partial t} = D \frac{\partial^2 u}{\partial x^2} \pm b \frac{\partial u}{\partial x}. \quad (49)$$

When deriving constant flux boundary conditions in the case of unbiased diffusion, the flux at  $x = 0$  was given by  $-Du_x$  in the diffusive limit, so we could implement constant flux boundary conditions with the Neumann boundary condition  $-Du_x = A$ . In the biased case, we must adapt our flux term to incorporate the directional bias so it is given by  $-Du_x + bu$  (assuming, without loss of generality, that the bias is towards rightward movement).

### 6.1. Local case

We begin by considering the local case, and write the master equation for the first lattice site, which includes particles being added to the system during timestep  $\Delta t$  with probability  $J\Delta t/h$ ,



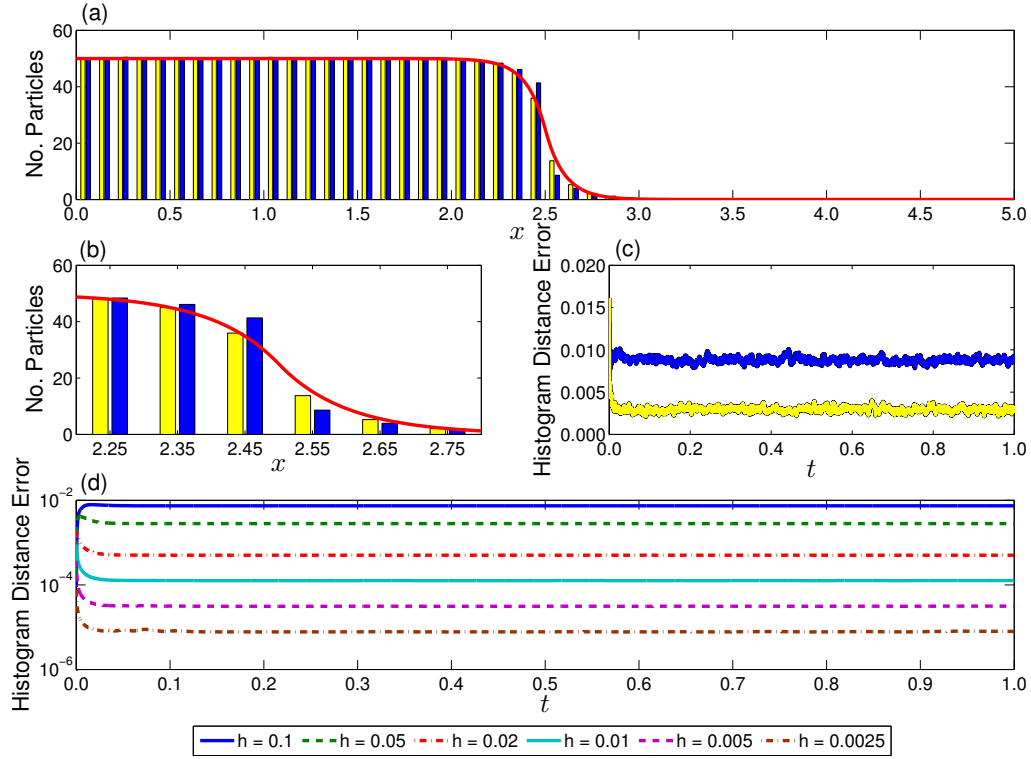


**Figure 9.** (a) shows the state of a morphogen gradient system at time  $t = 1$ , starting from an initial state with no particles anywhere, as described in section 5.2. Both simulations are non-local with  $Q = 5$ , but the results shown by yellow bars were obtained using the hybrid method, with the interface positioned at  $x = 1.5$ , while the blue bars represent the standard non-local implementation. The red line shows the solution to the limiting PDE. It can be seen that the standard non-local simulations deviate slightly from the PDE solution around  $x = 2.5$ , and an enlarged image of this region is shown in (b). The goodness of fit of the hybrid method to the PDE solution is shown by the comparison of HDEs in (c). Another approach to sharp gradients is to adopt a finer lattice, and in (d) we see the solution of the master equations describing the non-local morphogen gradient system becoming closer to the solution of the limiting PDE as  $h$  becomes smaller, without requiring a hybrid method.

$$m_1(t + \Delta t) = \left(1 - D\frac{\Delta t}{h^2} - b\frac{\Delta t}{h}\right) m_1(t) + D\frac{\Delta t}{h^2} m_2(t) + J\frac{\Delta t}{h}, \quad (50)$$

$$\Rightarrow \sqrt{\Delta t} \frac{m_1(t + \Delta t) - m_1(t)}{\Delta t} = D \frac{\sqrt{\Delta t}}{h} \frac{m_2(t) - m_1(t)}{h} - b \frac{\sqrt{\Delta t}}{h} m_1(t) + J \frac{\sqrt{\Delta t}}{h}. \quad (51)$$

In the diffusive limit, the left-hand side goes to zero, and all  $\sqrt{\Delta t}/h$  terms tend to a constant and cancel. Therefore, we can rearrange to get

$$J = \left( -D \frac{\partial m(t)}{\partial x} + b m(t) \right) \Big|_{x=0} = A. \quad (52)$$

So the unbiased implementation also works for biased jumping in the local jumping case. When the bias is towards leftward movement, it is easy to produce the same result by a very similar method.

## 6.2. Non-local case

We assume the bias is away from the boundary at  $x = 0$ , and begin by deriving a result for the first box on the lattice, then proceed to derive results for the remaining  $Q - 1$  boxes. We then show that the sum of all the terms added as a result of directional bias is zero, so total flux is conserved. For the first box, we write the master equation,

$$\begin{aligned} \sqrt{\Delta t} \frac{m_1(t + \Delta t) - m_1(t)}{\Delta t} = & \frac{D\sqrt{\Delta t}}{Qh^2} \left\{ \left[ -\sum_{j=1}^Q \frac{1}{j^2} - \sum_{j=2}^Q \frac{1}{j^2} \right] m_1(t) \right. \\ & + \sum_{j=1}^Q \left[ \frac{1}{j^2} m_{j+1}(t) \right] + \sum_{j=2}^Q \left[ \frac{1}{j^2} m_j(t) \right] \Big\} \\ & - b \frac{\sqrt{\Delta t}}{h} m_1(t) + J_{1,Q} \frac{\sqrt{\Delta t}}{h}. \end{aligned} \quad (53)$$

We ignore the left-hand side, which will vanish in the diffusive limit. On the right-hand side, the four summations represent, respectively, particles leaving box 1 by jumping to the right, particles leaving box 1 by jumping to the left and reflecting, particles jumping directly into box 1 from the right, and particles jumping into box 1 from the right by reflection. The terms outside of the brackets represent advection to the right and flux into the box from outside the system.

In our earlier work, we showed that the terms inside the brackets can be rearranged, collecting most into second derivative terms which vanish in the diffusive limit, and leaving

$$0 = \frac{D}{Q} \left( \sum_{j=1}^Q \frac{2j-1}{j^2} \right) \frac{\partial u}{\partial x} \Big|_{x=0} - bu(0, t) + J_{1,Q}. \quad (54)$$

Recalling the expression for flux in the advective case, we rearrange this to write

$$J_{1,Q} = \frac{1}{Q} \left( \sum_{j=1}^Q \frac{2j-1}{j^2} \right) \left[ -D \frac{\partial u}{\partial x} \Big|_{x=0} + bu(0, t) \right] + \left( 1 - \frac{1}{Q} \left( \sum_{j=1}^Q \frac{2j-1}{j^2} \right) \right) bu(0, t). \quad (55)$$

We therefore apply our boundary condition to arrive at

$$J_{1,Q} = \frac{1}{Q} \left( \sum_{j=1}^Q \frac{2j-1}{j^2} \right) A + \left( 1 - \frac{1}{Q} \left( \sum_{j=1}^Q \frac{2j-1}{j^2} \right) \right) bu(0, t). \quad (56)$$

### 6.3. All other boxes

For some box  $k$ , where  $1 < k \leq Q$ , we can apply similar reasoning, drawing on our previous work to write

$$0 = \frac{D}{Q} \left( \sum_{j=k}^Q \frac{2j-2k+1}{j^2} \right) \frac{\partial u}{\partial x} \Big|_{x=0} - b\sqrt{\Delta t} \frac{\partial u}{\partial x} + J_{1,Q} \frac{\sqrt{\Delta t}}{h}. \quad (57)$$

Having rearranged the bias terms into a first order derivative they vanish in the diffusive limit. In order to get an expression for flux at the boundary, we include balancing terms of  $m_1$  in the equation, and arrive at our final expression for flux,

$$J_{k,Q} = \frac{1}{Q} \left( \sum_{j=k}^Q \frac{2j-2k+1}{j^2} \right) A - \frac{1}{Q} \left( \sum_{j=k}^Q \frac{2j-2k+1}{j^2} \right) bu(0, t). \quad (58)$$

We note that in the case  $b = 0$  we recover our unbiased result. Drawing on our earlier work on boundary conditions, it can be seen that the sum of the advection-dependent terms over all the boxes will be zero, so we can see that the flux at the boundary is still conserved when there is a bias in the jump rates. We also note that the new terms are independent of the boundary flux  $A$ . They will therefore need to be incorporated into the system even for zero-flux boundary conditions where  $A = 0$ , or when a different boundary condition is implemented: it is easy to see that these terms are also required for Robin boundary conditions. It therefore seems sensible,

both for computational efficiency and for accurate particle numbers, to implement these terms as extra jumps between the first  $Q$  boxes, i.e. where these terms call for particles to be removed from the system, they should instead be moved to one of the sites (chosen with appropriate probability) where the additional terms require particles to be added. We note that if the bias instead favours movement towards the boundary then the signs of these extra terms will all be flipped.

#### 6.4. Example

To demonstrate the necessity for additional boundary flux terms for biased diffusion, we ran 2,000 simulations of a biased system with  $Q = 5$ . In 1,000 of these simulations we used the flux values derived above for biased diffusion (shown as yellow bars in figure 10(c)) using  $m_1(t)$  to approximate  $u(0, t)$ , while in the other 1,000 we used the standard, non-local flux implementation for unbiased diffusion (shown in blue). An in-flux boundary condition with  $A = -500$  was set at  $x = 0$ , and an outflux condition with  $A = -500$  at  $x = 5$ . We use  $D = 1$  as usual, and a bias towards rightward movement of  $b = 5$ . The simulations started from the steady state, with 5,000 particles distributed uniformly across the domain as shown in figure 10(a). Figure 10(c) shows the average state of the system at  $t = 1$ , with the unbiased boundary conditions giving rise to a density profile that deviates significantly from the steady state (red line). This illustrates the need to derive boundary conditions for biased diffusion, and when these are used our results correspond well to the steady state. The quality of the fit is confirmed in figure 10(b) by comparison of the HDEs. The non-local simulations ran in an average of 64.0 seconds, compared to 137.8 seconds for an equivalent, local simulation. Non-local jumping can therefore still deliver significant, albeit smaller, savings in computational time, even when more complicated boundary condition implementations are required. It can also be seen, in figure 10(d), that the non-local description converges to the solution of the continuum PDE as  $h$  becomes small.

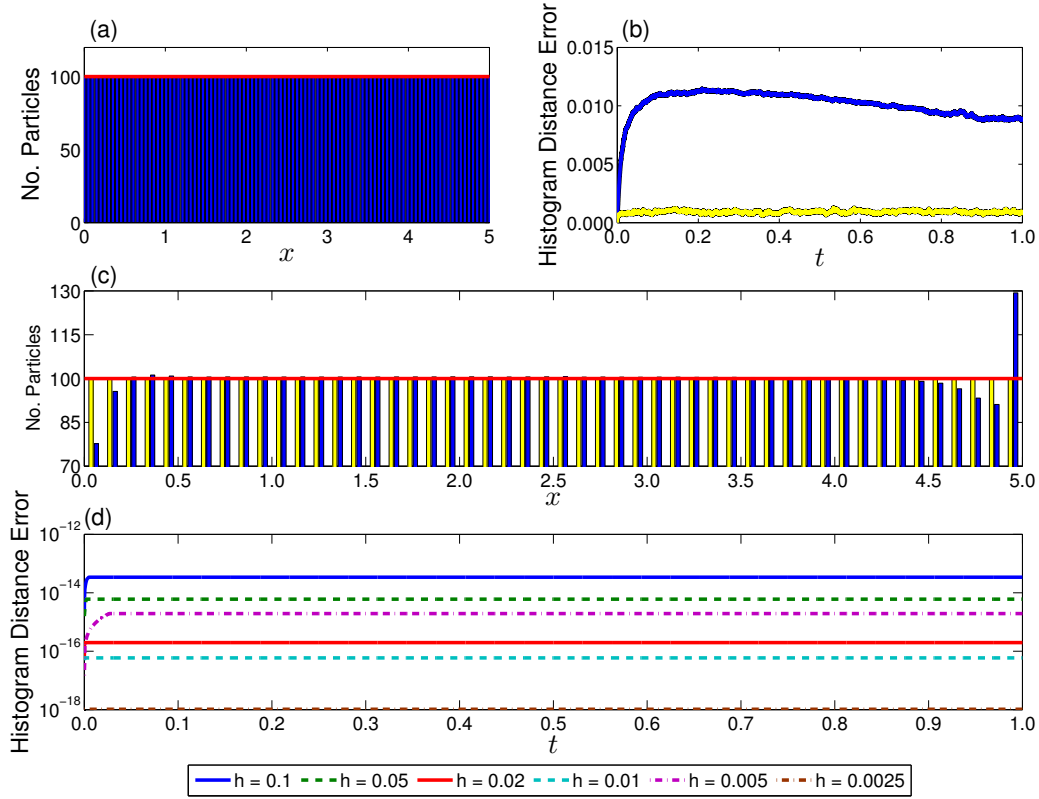


**Figure 10.** (a) shows the initial state of the system (and also the steady state) with 100 particles in each box, as described in section 6.4. A comparison of HDEs for the derived asymmetric boundary conditions (yellow) and standard non-local boundary conditions (blue) is shown in (b), demonstrating the accuracy of the asymmetric implementation. In (c), the average state of the system at time  $t$  is shown: it can be seen that particles numbers around the boundary deviate significantly from the steady state (red line), while the asymmetric implementation matches the steady state well. As  $h$  becomes smaller, we see in (d) that the solution of the master equations describing the biased diffusion system with boundary fluxes becomes closer to the solution of the limiting PDE.

### 6.5. Robin boundaries for biased jumping

Recalling our notation from section 3, we choose to let particles which hit the boundary as a result of the biased jumping term  $b\Delta t/h$  be absorbed with probability  $P_{1,Q}$ , while particles hitting the boundary because of a diffusive term are still adsorbed with probability  $P_{1,Q}h$  as before. It is necessary for the probability of adsorption from

diffusive jumping to scale with  $h$  since such jumps scale with  $\Delta t/h^2$ , whereas the biased jumping terms scale with  $\Delta t/h$ . The terms describing adsorption from biased jumping would therefore vanish in the diffusive limit if their adsorption probability scaled with  $h$ . Using the reasoning from section 6.1, and noting that the non-local Robin condition at the left-hand boundary is  $D\partial u/\partial x + bm = Ru$  if the bias is towards leftward movement, and  $D\partial u/\partial x - bu = Ru$  if towards rightward movement, it is easy to see that the local implementation of Robin conditions is unchanged at  $P_{1,1} = R/D$  when the bias moves particles away from the boundary, and  $P_{1,1} = R/(D + b)$  when the bias moves them towards the boundary.

In the non-local case, we recall that the additional terms derived in sections 6.2 and 6.3 must also be incorporated here, but when the bias favours movement away from the boundary it is clear that the adsorption terms will remain unchanged. When movement towards the boundary is favoured by the bias, adsorption rates  $P_{k,Q}$  remain unchanged for  $k \geq 2$ , and it can be shown that for  $k = 1$  the result derived in (30) becomes instead

$$P_{1,Q} + \frac{bQ}{D}P_{1,Q} + \sum_{j=2}^Q \left[ \frac{P_{j,Q}}{j^2} \right] = \frac{R}{D} \sum_{j=1}^Q \left[ \frac{2j-1}{j^2} \right]. \quad (59)$$

Using the same reasoning applied to the symmetric case, we obtain our new value for  $P_{1,Q}$ :

$$P_{1,Q} = \frac{R}{D + bQ} \left( 1 + \sum_{j=2}^Q \left[ \frac{2}{j^2} \right] \right). \quad (60)$$

We note that this result preserves the symmetric rates when  $b = 0$  as expected. A lower adsorption rate also makes intuitive sense in this context. Our value of  $R$  is parametrising the proportion of particles in each of the first  $Q$  boxes which should be adsorped over a short time period, and this proportion is unchanged by the introduction of advection terms into the master equation. When the bias favours movement away from the boundary, the number of particles in the first box which hit the boundary and have a chance of being adsorped remains the same, but when the bias moves particles towards the boundary there will be more reflecting particles. In order to keep the proportion of particles adsorped from the box constant, the adsorption rate is

therefore be lower when advection moves particles towards the boundary, but unchanged otherwise.

To illustrate this result we ran 1,000 simulations, using the same parameters, and the same initial condition, as used in figure 4, except for the addition of a bias towards leftward movement with  $b = 2$ . It can be seen in figure 11 that our derived modifications to the adsorption rates result in a good match to the PDE solution by both local and non-local simulations. Each non-local jumping simulation ran in an average of 8.8 seconds, compared to an average of 23.8 seconds, showing that, even in this complicated case, non-local jumping can accelerate stochastic simulations of LBPJ models. Figure 11(d) shows the convergence of the non-local system to the limiting PDE for small  $h$ .

## 7. Discussion

Computational time can provide a barrier to the use of exact stochastic algorithms such as the Gillespie algorithm and its extensions. This is especially true for variants of the inhomogeneous stochastic simulation algorithm, where a spatially-inhomogeneous chemical reaction system is modelled as a collection of well-mixed subsystems that particles can diffuse between and react within. A number of adaptations have been proposed to accelerate the simulation of systems where diffusion events occur much more frequently than reaction events, such as the multinomial simulation algorithm [19]. Other developments include adaptive mesh refinements to focus computational resources efficiently on important regions of the lattice [20]. Our non-local diffusion model suggests a new avenue of research in this regard, by reducing computational time, as illustrated by comparisons throughout this article, while retaining the option of tracking individual particles, and remaining relatively simple to implement and explain. These time savings arise from the need to simulate fewer diffusion events, which outweighs the increased number of possible events to be checked, at least when implemented in an efficiently sorted, next subvolume method style algorithm [21].

We have presented a framework for using non-local jumping to accelerate stochastic

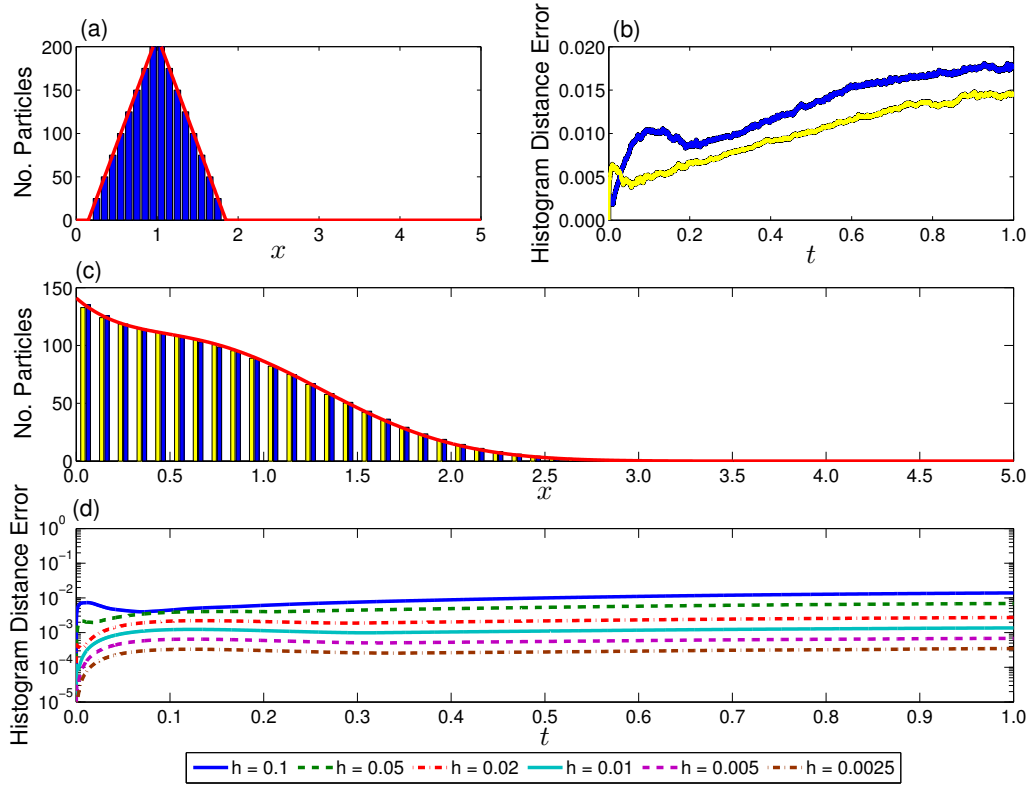


**Figure 11.** (a) shows the initial state of the system (and the steady state) with 1800 particles placed in a peaked profile about  $x = 1$ , as described in section 6.5. In (c) we see the averaged system state at time  $t = 0.2$ , averaged over 1,000 simulations, with a good match between both local (blue bars) and non-local (yellow bars) simulations, and the PDE solution (red line). The HDEs confirm this match in (b) their rising values resulting from the rapidly dropping number of particles in the system. In (d) we see the solution of the master equations describing the biased diffusion system with Robin boundary condition becoming closer to the solution of the limiting PDE as  $h$  becomes smaller.

diffusion simulations, developing the initial theory to incorporate hybrid systems and asymmetric jumping. We have also derived generalised boundary conditions for local and non-local jumping, corresponding to flux and Robin boundary conditions in the diffusive limit. Simulations have demonstrated the accuracy with which these models correspond to their locally, jumping and PDE equivalents, and have also shown the time-saving potential these methods offer. In future work we will extend our implementation to two-dimensional diffusion systems, and anticipate that the use of binary searching will



allow reductions in computational time to be maintained despite the greatly increased number of possible jump events for a non-local system in higher dimensions. We also intend to rigourously justify the incorporation of higher order reactions, following recent work on the convergence of the reaction-diffusion master equation [22], and to study other jump length distributions which satisfy the condition given by (5).

## **Acknowledgments**

PRT would like to thank the UK's Engineering and Physical Sciences Research Council (EPSRC) for funding through a studentship at the Systems Biology programme of the University of Oxford's Doctoral Training Centre. CAY would like to thank Christ Church, Oxford for a Junior Research Fellowship. The authors are grateful to Philip Maini and two anonymous reviewers for helpful comments on drafts of this paper.

## Appendix A. Proofs by induction: reflecting terms

In this and the two following appendices, we apply the same method: we write each expression so that all terms are grouped with some variable  $m_i(t)$ , then we take the highest value of  $i$  and rearrange all  $m_i(t)$  terms, along with the appropriate values of  $m_{i-1}$  and  $m_{i-2}(t)$ , into a second derivative which will vanish in the diffusive limit. This step is repeated until only terms of  $m_1(t)$  and  $m_2(t)$  have not been rearranged into second derivatives.

*Appendix A.1. Case when  $k = 1$*

$$\frac{D\sqrt{\Delta t}}{Qh^2} \left\{ - \left[ \sum_{j=2}^Q \frac{1}{j^2} \right] m_1(t) + \sum_{j=2}^Q \left[ \frac{1}{j^2} m_j(t) \right] \right\}. \quad (\text{A.1})$$

We apply the method described above, removing one variable at a time by rearranging it into a second derivative which will vanish in the diffusive limit. To begin the proof by induction, we assume that after  $s \leq Q - 4$  steps of this method the expression will be of the form

$$\begin{aligned} & \frac{D\sqrt{\Delta t}}{Qh^2} \left\{ - \left[ \sum_{j=2}^Q \frac{1}{j^2} \right] m_1(t) + \sum_{j=2}^{Q-s-2} \left[ \frac{1}{j^2} m_j(t) \right] \right. \\ & + \left[ \frac{1}{(Q-s-1)^2} - \sum_{j=Q-s+1}^Q \left[ \frac{j-Q+s}{j^2} \right] \right] m_{Q-s-1}(t) \\ & + \left[ \sum_{j=Q-s}^Q \left[ \frac{j-Q+s+1}{j^2} \right] \right] m_{Q-s}(t) \\ & \left. + h^2 \sum_{j=Q-s+1}^Q \left[ \sum_{i=j}^Q \left[ \frac{i-j+1}{i^2} \right] \frac{(m_{j-2}(t) - 2m_{j-1}(t) + m_j(t))}{h^2} \right] \right\}. \quad (\text{A.2}) \end{aligned}$$

Assume this conjecture holds true for some value of  $s$ , then rearrange so that  $m_{Q-s}$  is only present inside a second derivative term, i.e.

$$\begin{aligned} & \frac{D\sqrt{\Delta t}}{Qh^2} \left\{ - \left[ \sum_{j=2}^Q \frac{1}{j^2} \right] m_1(t) + \sum_{j=2}^{Q-s-3} \left[ \frac{1}{j^2} m_j(t) \right] \right. \\ & \left[ \frac{1}{(Q-s-2)^2} - \sum_{j=Q-s}^Q \left[ \frac{j-Q+s+1}{j^2} \right] \right] m_{Q-s-2}(t) \end{aligned}$$

$$\begin{aligned}
& \left[ \frac{1}{(Q-s-1)^2} + 2 \sum_{j=Q-s}^Q \left[ \frac{j-Q+s+1}{j^2} \right] - \sum_{j=Q-s+1}^Q \left[ \frac{j-Q+s}{j^2} \right] \right] m_{Q-s-1}(t) \\
& + h^2 \sum_{j=Q-s}^Q \left[ \frac{j-Q+s+1}{j^2} \right] \left( \frac{m_{Q-s-2}(t) - 2m_{Q-s-1}(t) + m_{Q-s}(t)}{h^2} \right) \\
& + h^2 \sum_{j=Q-s+1}^Q \left[ \sum_{i=j}^Q \left[ \frac{i-j+1}{i^2} \right] \frac{(m_{j-2}(t) - 2m_{j-1}(t) + m_j(t))}{h^2} \right] \Bigg\}. \tag{A.3}
\end{aligned}$$

It is clear that the first and second lines match our conjecture for  $s+1$ , while the fourth line can be incorporated into the fifth to satisfy our conjecture again. Checking the coefficients of the third line then, we find

$$\begin{aligned}
& \frac{1}{(Q-s-1)^2} + 2 \sum_{j=Q-s}^Q \left[ \frac{j-Q+s+1}{j^2} \right] - \sum_{j=Q-s+1}^Q \left[ \frac{j-Q+s}{j^2} \right] \\
& = \frac{1}{(Q-s-1)^2} + 2 \frac{1}{(Q-s)^2} + \sum_{j=Q-s+1}^Q \left[ \frac{j-Q+s+2}{j^2} \right] \\
& = \sum_{j=Q-s-1}^Q \left[ \frac{j-Q+s+2}{j^2} \right], \tag{A.4}
\end{aligned}$$

which matches our conjecture. We complete our proof by induction by noting that our conjecture is true for  $s=1$ . We can then use it by setting  $s=Q-4$ , the last value for which our induction is valid due to the summation from  $j=2$  to  $Q-s-2$ , to arrive at the expression

$$\begin{aligned}
& \frac{D\sqrt{\Delta t}}{Qh^2} \left\{ - \left[ \sum_{j=2}^Q \frac{1}{j^2} \right] m_1(t) + \frac{1}{2^2} m_2(t) \right. \\
& + \left( \frac{1}{3^2} - \sum_{j=5}^Q \left[ \frac{j-4}{j^2} \right] \right) m_3(t) + \left( \sum_{j=4}^Q \left[ \frac{j-3}{j^2} \right] \right) m_4(t) \\
& \left. + h^2 \sum_{j=5}^Q \left[ \sum_{i=j}^Q \left[ \frac{i-j+1}{i^2} \right] \frac{(m_{j-2}(t) - 2m_{j-1}(t) + m_j(t))}{h^2} \right] \right\}. \tag{A.5}
\end{aligned}$$

Twice more we rearrange this term to form second derivatives, leaving an expression entirely in terms of  $m_1(t)$  and  $m_2(t)$ ,

$$\begin{aligned}
& = \frac{D\sqrt{\Delta t}}{Qh^2} \left\{ - \left[ \sum_{j=2}^Q \frac{1}{j^2} \right] m_1(t) + \left( \frac{1}{2^2} - \sum_{j=4}^Q \left[ \frac{j-3}{j^2} \right] \right) m_2(t) \right. \\
& + \left( \sum_{j=3}^Q \left[ \frac{j-2}{j^2} \right] \right) m_3(t)
\end{aligned}$$

$$+h^2 \sum_{j=4}^Q \left[ \sum_{i=j}^Q \left[ \frac{i-j+1}{i^2} \right] \frac{(m_{j-2}(t) - 2m_{j-1}(t) + m_j(t))}{h^2} \right] \Bigg\}, \quad (\text{A.6})$$

$$= \frac{D\sqrt{\Delta t}}{Qh^2} \left\{ - \left( \sum_{j=2}^Q \left[ \frac{1}{j^2} \right] + \sum_{j=3}^Q \left[ \frac{j-2}{j^2} \right] \right) m_1(t) + \left( \sum_{j=2}^Q \left[ \frac{j-1}{j^2} \right] \right) m_2(t) \right. \\ \left. + h^2 \sum_{j=3}^Q \left[ \sum_{i=j}^Q \left[ \frac{i-j+1}{i^2} \right] \frac{(m_{j-2}(t) - 2m_{j-1}(t) + m_j(t))}{h^2} \right] \right\}. \quad (\text{A.7})$$

Taking the diffusive limit, all the second derivative terms go to zero, while  $m_1(t)$  and  $m_2(t)$  form a first derivative, so that (A.7) simplifies to

$$\frac{D\sqrt{\Delta t}}{Qh} \left( \sum_{j=2}^Q \left[ \frac{j-1}{j^2} \right] \right) \left( \frac{m_2(t) - m_1(t)}{h} \right). \quad (\text{A.8})$$

In the diffusive limit this becomes

$$\frac{D}{Q} \left( \sum_{j=2}^Q \left[ \frac{j-1}{j^2} \right] \right) \frac{\partial u}{\partial x} \Big|_{x=0}. \quad (\text{A.9})$$

#### Appendix A.2. Case when $k > 1$ , but $2k - 1 \geq Q$

We begin by noting that  $2k - 1$  is the length of jump required for a particle to travel left from box  $k$  and be returned to the same box by reflection. We therefore begin by considering the case  $2k - 1 \geq Q$ , where only boxes to the left of  $x_k$  will contribute reflecting particles to the total number in  $k$ , and later combine this with the case  $2k - 1 < Q$ , where we must also consider particles reflecting into box  $k$  which started from boxes to the right.

We therefore begin by considering the following reflecting terms,

$$\frac{D\sqrt{\Delta t}}{Qh^2} \left\{ \sum_{j=1}^{Q-k+1} \left[ \frac{1}{(j+k-1)^2} m_j(t) \right] - \left[ \sum_{j=1}^{Q-k+1} \frac{1}{(j+k-1)^2} \right] m_k(t) \right\}. \quad (\text{A.10})$$

If  $Q < 2k - 2$  then there will be values of  $l$ ,  $Q - k + 1 < l < k$ , such that the coefficients of  $m_l(t)$  are zero. We then use our established iteration  $2k - 1 - Q$  times, so that all remaining  $m$  terms from  $m_1(t)$  to  $m_{Q-k+1}$  have non-zero coefficients, i.e.

$$\frac{D\sqrt{\Delta t}}{Qh^2} \left\{ \sum_{j=1}^{Q-k-1} \left[ \frac{1}{(j+k-1)^2} m_j(t) \right] \right. \\ \left. + \left[ \frac{1}{(Q-1)^2} - (2k-Q-1) \sum_{j=1}^{Q-k+1} \frac{1}{(j+k-1)^2} \right] m_{Q-k}(t) \right\}$$

$$- \left[ \frac{1}{Q^2} - (2k - Q) \sum_{j=1}^{Q-k+1} \frac{1}{(j+k-1)^2} \right] m_{Q-k+1}(t) \Bigg\}. \quad (\text{A.11})$$

In the case  $Q = k - 1$  this yields

$$\frac{D}{Q} \left\{ \frac{(k-1)}{k^2} + \frac{k-2}{(k+1)^2} \right\} \frac{\partial m}{\partial x} \Big|_{x=0}. \quad (\text{A.12})$$

Otherwise, after a further  $Q - k - 1$  iterations, we have

$$\begin{aligned} & \frac{D\sqrt{\Delta t}}{Qh^2} \left\{ \left[ \frac{1}{k^2} - \sum_{j=3}^{Q-k+1} \left[ \frac{j-2}{(j+k-1)^2} \right] + (k-2) \sum_{j=1}^{Q-k+1} \left[ \frac{1}{(j+k-1)^2} \right] \right] m_1(t) \right. \\ & \left. - \left[ \frac{1}{(k+1)^2} + \sum_{j=3}^{Q-k+1} \left[ \frac{j-1}{(j+k-1)^2} \right] - (k-1) \sum_{j=1}^{Q-k+1} \left[ \frac{1}{(j+k-1)^2} \right] \right] m_2(t) \right\}. \quad (\text{A.13}) \end{aligned}$$

In the diffusive limit this becomes

$$\frac{D}{Q} \left( \sum_{j=k}^Q \left[ \frac{j-2k+1}{j^2} \right] \right) \frac{\partial u}{\partial x} \Big|_{x=0}, \quad (\text{A.14})$$

which is consistent with our result for  $k = 1$ .

### Appendix A.3. Case when $k > 1$ , but $2k - 1 < Q$

Considering the case where  $2k - 1 < Q$ , the contribution of reflection to the master equation can be divided into two parts,

$$\begin{aligned} & \frac{D\sqrt{\Delta t}}{Qh^2} \left\{ \sum_{j=1}^k \left[ \frac{1}{(j+k-1)^2} m_j(t) \right] - \left[ \sum_{j=1}^k \frac{1}{(j+k-1)^2} \right] m_k(t) \right. \\ & \left. - \left[ \sum_{j=k+1}^{Q-k+1} \frac{1}{(j+k-1)^2} \right] m_k(t) + \sum_{j=k+1}^{Q-k+1} \left[ \frac{1}{(j+k-1)^2} m_j(t) \right] \right\}. \quad (\text{A.15}) \end{aligned}$$

From our previous result, it is clear that the first line of this expression will end up contributing

$$\frac{D}{Q} \left( \sum_{j=k}^{2k-1} \frac{j-2k+1}{j^2} \right) \frac{\partial u}{\partial x} \Big|_{x=0}, \quad (\text{A.16})$$

to the value of  $B_k$ , so we can concentrate on the second line. After  $Q - 2k$  iterations, this can be reduced to

$$- \left[ \sum_{j=k+1}^{Q-k+1} \left[ \frac{1}{(j+k-1)^2} \right] + \sum_{j=2k+1}^Q \left[ \frac{j-2k}{j^2} \right] \right] m_k(t) + \left[ \sum_{j=2k}^Q \left[ \frac{j-2k+1}{j^2} \right] \right] m_{k+1}(t). \quad (\text{A.17})$$

After a further  $k - 1$  iterations, all terms of  $m_i$ ,  $i > 2$ , have been rearranged into second derivatives and will vanish in the diffusive limit. We are left with

$$\begin{aligned} \frac{D\sqrt{\Delta t}}{Qh^2} \left\{ - \left[ (k-1) \sum_{j=2k}^Q \left[ \frac{j-2k+1}{j^2} \right] - (k-2) \sum_{j=2k+1}^Q \left[ \frac{j-2k}{j^2} \right] \right. \right. \\ \left. - (k-2) \sum_{j=k+1}^{Q-k+1} \left[ \frac{1}{(j+k-1)^2} \right] \right] m_1(t) \\ + \left[ k \sum_{j=2k}^Q \left[ \frac{j-2k+1}{j^2} \right] - (k-1) \sum_{j=2k+1}^Q \left[ \frac{j-2k}{j^2} \right] \right. \\ \left. - (k-1) \sum_{j=k+1}^{Q-k+1} \left[ \frac{1}{(j+k-1)^2} \right] \right] m_2(t) \left. \right\}. \end{aligned} \quad (\text{A.18})$$

After rearranging and taking the diffusive limit, it can be seen that the expression resolves to

$$\frac{D}{Q} \sum_{j=2k}^Q \left[ \frac{j-2k+1}{j^2} \right] \frac{\partial u}{\partial x} \Big|_{x=0}. \quad (\text{A.19})$$

Adding the terms from (A.16) and (A.19), we obtain

$$\frac{D}{Q} \sum_{j=k}^Q \left[ \frac{j-2k+1}{j^2} \right] \frac{\partial u}{\partial x} \Big|_{x=0}, \quad (\text{A.20})$$

which has been shown to hold for all values of  $k$ .

## Appendix B. Proofs by induction: non-reflecting terms

### Appendix B.1. Case when $k = 1$

The non-reflecting jumping terms relative to the first lattice box are given by

$$\frac{D\sqrt{\Delta t}}{Qh^2} \left\{ - \left[ \sum_{j=1}^Q \frac{1}{j^2} \right] m_1(t) + \sum_{j=1}^Q \left[ \frac{1}{j^2} m_{j+1}(t) \right] \right\}. \quad (\text{B.1})$$

As in Appendix A, the  $m_{Q+1}(t)$  term can be removed from this expression by rearranging it, together with some other terms, into a second derivative, which will vanish as  $\Delta t \rightarrow 0$ .

The resulting expression is given by

$$\begin{aligned} \frac{D\sqrt{\Delta t}}{Qh^2} \left\{ - \left[ \sum_{j=1}^Q \frac{1}{j^2} \right] m_1(t) + \sum_{j=1}^{Q-3} \left[ \frac{1}{j^2} m_{j+1}(t) \right] + \left[ \frac{1}{(Q-2)^2} - \frac{1}{Q^2} \right] m_{Q-1}(t) \right. \\ \left. + \left[ \frac{1}{(Q-1)^2} + 2\frac{1}{Q^2} \right] m_Q(t) \right\} \end{aligned}$$

$$+ \left( \frac{1}{Q^2} \frac{D\sqrt{\Delta t}}{Q} \frac{m_{Q-1}(t) - 2m_Q(t) + m_{Q+1}(t)}{h^2} \right). \quad (\text{B.2})$$

This is the the expression after one step (i.e. the conversion of the last term into a second derivative) so we conjecture that after  $s$  steps, for  $s \leq (Q - 3)$ , it will be of the form

$$\begin{aligned} & \frac{D\sqrt{\Delta t}}{Qh^2} \left\{ - \left[ \sum_{j=1}^Q \frac{1}{j^2} \right] m_1(t) + \sum_{j=1}^{Q-s-2} \left[ \frac{1}{j^2} m_{j+1}(t) \right] \right. \\ & + \left[ \frac{1}{(Q-s-1)^2} - \sum_{j=Q-s+1}^Q \left( (j-Q+s) \frac{1}{j^2} \right) \right] m_{Q-s}(t) \\ & + \left. \left[ \sum_{j=Q-s}^Q (j-Q+s+1) \frac{1}{j^2} \right] m_{Q-s+1}(t) \right\} \\ & + \frac{D\sqrt{\Delta t}}{Q} \sum_{j=Q-s+1}^Q \left( \sum_{i=j}^Q \left[ \frac{i-j+1}{i^2} \right] \frac{m_{j-1}(t) - 2m_j(t) + m_{j+1}(t)}{h^2} \right), \end{aligned} \quad (\text{B.3})$$

where the terms on the last line will vanish in the diffusive limit. This holds for  $s = 1$ , so we use a proof by induction again (not shown here). The next step is to remove the  $m_{Q-s+1}(t)$  term by separating it out into another vanishing second derivative, so the expression becomes

$$\begin{aligned} & \frac{D\sqrt{\Delta t}}{Qh^2} \left\{ - \left[ \sum_{j=1}^Q \frac{1}{j^2} \right] m_1(t) + \sum_{j=1}^{Q-s-3} \left[ \frac{1}{j^2} m_{j+1}(t) \right] \right. \\ & + \left[ \frac{1}{(Q-s-2)^2} - \sum_{j=Q-s}^Q \left( (j-Q+s+1) \frac{1}{j^2} \right) \right] m_{Q-s-1}(t) \\ & + \left[ \frac{1}{(Q-s-1)^2} - \sum_{j=Q-s+1}^Q \left( (j-Q+s) \frac{1}{j^2} \right) + 2 \sum_{j=Q-s}^Q \left( (j-Q+s+1) \frac{1}{j^2} \right) \right] m_{Q-s}(t) \Big\} \\ & + \left( \sum_{j=Q-s}^Q (j-Q+s+1) \frac{1}{j^2} \frac{D\sqrt{\Delta t}}{Q} \frac{m_{Q-s-1}(t) - 2m_{Q-s}(t) + m_{Q-s+1}(t)}{h^2} \right) \\ & + \frac{D\sqrt{\Delta t}}{Q} \sum_{j=Q-s+1}^Q \left( \sum_{i=j}^Q \left[ \frac{i-j+1}{i^2} \right] \frac{m_{j-1}(t) - 2m_j(t) + m_{j+1}(t)}{h^2} \right). \end{aligned} \quad (\text{B.4})$$

It is clear that the first and second lines of this expression recapitulate the postulated general form after  $s + 1$  steps, as do the fourth and fifth when taken in combination.

Rearranging the coefficients of  $m_{Q-s}$ , we can rewrite them as

$$\frac{1}{(Q-s-1)^2} + \sum_{j=Q-s+1}^Q \left[ -(j-Q+s) \frac{1}{j^2} + 2(j-Q+s+1) \frac{1}{j^2} \right] + 2 \frac{1}{(Q-s)^2}$$

$$\begin{aligned}
&= \frac{1}{(Q-s-1)^2} + 2\frac{1}{(Q-s)^2} + \sum_{j=Q-s+1}^Q \left[ (j-Q+s+2) \frac{1}{j^2} \right] \\
&= \sum_{j=Q-s-1}^Q \left[ (j-Q+s+2) \frac{1}{j^2} \right], \tag{B.5}
\end{aligned}$$

which matches the general form again, completing our proof by induction. When

$s = Q - 3$ , we can write

$$\begin{aligned}
&\frac{D\sqrt{\Delta t}}{Qh^2} \left\{ - \left[ \sum_{j=1}^Q \frac{1}{j^2} \right] m_1(t) + \frac{1}{1^2} m_2(t) + \left( \frac{1}{2^2} - \sum_{j=4}^Q \left[ \frac{j-3}{j^2} \right] \right) m_3(t) + \left( \sum_{j=3}^Q \left[ \frac{j-2}{j^2} \right] \right) m_4(t) \right\} \\
&+ \frac{D\sqrt{\Delta t}}{Q} \sum_{j=4}^Q \left( \sum_{i=j}^Q \left[ \frac{i-j+1}{i^2} \right] \frac{m_{j-1}(t) - 2m_j(t) + m_{j+1}(t)}{h^2} \right), \tag{B.6}
\end{aligned}$$

and hence remove  $m_4(t)$  from the expression as before, subsuming it into the second derivative term,

$$\begin{aligned}
&\frac{D\sqrt{\Delta t}}{Qh^2} \left\{ - \left[ \sum_{j=1}^Q \frac{1}{j^2} \right] m_1(t) + \left[ \frac{1}{1^2} - \sum_{j=3}^Q \left[ \frac{j-2}{j^2} \right] \right] m_2(t) \right. \\
&+ \left. \left( \frac{1}{2^2} - \sum_{j=4}^Q \left[ \frac{j-3}{j^2} \right] + 2 \sum_{j=3}^Q \left[ \frac{j-2}{j^2} \right] \right) m_3(t) \right\} \\
&+ \frac{D\sqrt{\Delta t}}{Q} \sum_{j=3}^Q \left( \sum_{i=j}^Q \left[ \frac{i-j+1}{i^2} \right] \frac{m_{j-1}(t) - 2m_j(t) + m_{j+1}(t)}{h^2} \right). \tag{B.7}
\end{aligned}$$

Noting that the coefficients of  $m_3(t)$  can be consolidated as  $\sum_{j=2}^Q [j-1]/Q$  we then do the same to  $m_3(t)$  and are left with an expression in terms of  $m_1(t)$  and  $m_2(t)$  alone:

$$\begin{aligned}
&\frac{D\sqrt{\Delta t}}{Qh^2} \left\{ - \left[ \sum_{j=1}^Q \left( \frac{1}{j^2} \right) + \sum_{j=2}^Q \left( \frac{j-1}{j^2} \right) \right] m_1(t) \right. \\
&+ \left. \left[ \frac{1}{1^2} - \sum_{j=3}^Q \left[ \frac{j-2}{j^2} \right] + 2 \sum_{j=2}^Q \left( \frac{j-1}{j^2} \right) \right] m_2(t) \right\} \\
&+ \frac{D\sqrt{\Delta t}}{Q} \sum_{j=2}^Q \left( \sum_{i=j}^Q \left[ \frac{i-j+1}{i^2} \right] \frac{m_{j-1}(t) - 2m_j(t) + m_{j+1}(t)}{h^2} \right). \tag{B.8}
\end{aligned}$$

Then rearranging, and discarding the second derivative terms completely, gives us

$$\frac{D\sqrt{\Delta t}}{Qh} \left( \sum_{j=1}^Q \frac{1}{j} \right) \left( \frac{m_2(t) - m_1(t)}{h} \right), \tag{B.9}$$

so in the diffusive limit, keeping the ratio  $\sqrt{\Delta t}/h$  constant, we arrive at

$$\frac{D}{Q} \left( \sum_{j=1}^Q \frac{1}{j} \right) \frac{\partial u}{\partial x} \Big|_{x=0}. \tag{B.10}$$



Appendix B.2. Case when  $k \neq 1$ 

Having found this expression for the first box, we now generalise this to derive an expression for the  $k^{\text{th}}$  box. The relevant expressions are

$$\begin{aligned} & \frac{D\sqrt{\Delta t}}{Qh^2} \left\{ \left( \sum_{j=1}^{k-1} \frac{1}{(k-j)^2} m_j(t) \right) - \left( \sum_{j=1}^{k-1} \frac{1}{(k-j)^2} + \sum_{j=1}^Q \frac{1}{j^2} \right) m_k(t) \right. \\ & \left. + \sum_{j=1}^Q \left( \frac{1}{j^2} m_{k+j}(t) \right) \right\}, \end{aligned} \quad (\text{B.11})$$

where the four summations represent particles jumping in from the left, out to the left, out to the right and in from the right, respectively.

We notice that, taken together, the terms for jumping in from and out to the right are the same as the whole expression for the first box, except defined for  $m_k$  and  $m_{k+j}$  rather than for  $m_1$  and  $m_{k+1}$ . We therefore know that after  $Q-1$  steps, using the same approach as before, these terms will reduce to

$$- \left( \sum_{j=1}^Q \frac{1}{j} \right) m_k(t) + \left( \sum_{j=1}^Q \frac{1}{j} \right) m_{k+1}(t), \quad (\text{B.12})$$

plus some second derivative terms which will vanish in the diffusive limit. Discarding these derivative terms for simplicity, the system becomes

$$\begin{aligned} & \frac{D\sqrt{\Delta t}}{Qh^2} \left\{ \left( \sum_{j=1}^{k-1} \frac{1}{(k-j)^2} m_j(t) \right) - \left( \sum_{j=1}^{k-1} \frac{1}{(k-j)^2} + \sum_{j=1}^Q \frac{1}{j} \right) m_k(t) \right. \\ & \left. + \sum_{j=1}^Q \left( \frac{1}{j} \right) m_{k+1}(t) \right\}. \end{aligned} \quad (\text{B.13})$$

Taking another step to eliminate  $m_{k+1}(t)$ , and discarding the resulting second derivative again, this becomes

$$\begin{aligned} 0 = & \frac{D\sqrt{\Delta t}}{Qh^2} \left\{ \left( \sum_{j=1}^{k-2} \frac{1}{(k-j)^2} m_j(t) \right) + \left( \frac{1}{1^2} - \sum_{j=1}^Q \frac{1}{j} \right) m_{k-1}(t) \right. \\ & \left. + \left( \sum_{j=1}^Q \frac{1}{j} - \sum_{j=1}^{k-1} \frac{1}{(k-j)^2} \right) m_k(t) \right\}. \end{aligned} \quad (\text{B.14})$$

In the case where  $k = 2$ , the first term is zero, and in the diffusive limit this expression becomes

$$\frac{D}{Q} \left( \sum_{j=2}^Q \frac{1}{j} \right) \frac{\partial u}{\partial x} \Big|_{x=0}. \quad (\text{B.15})$$

After another iteration of the method we get the expression (discarding the second derivative again),

$$0 = \frac{D\sqrt{\Delta t}}{Qh^2} \left\{ \left( \sum_{j=1}^{k-3} \frac{1}{(k-j)^2} m_j(t) \right) + \left( \frac{1}{2^2} - \sum_{j=1}^Q \frac{1}{j} + \sum_{j=1}^{k-1} \frac{1}{(k-j)^2} \right) m_{k-2}(t) \right. \\ \left. + \left( \frac{1}{1^2} + \sum_{j=1}^Q \frac{1}{j} - 2 \sum_{j=1}^{k-1} \frac{1}{(k-j)^2} \right) m_{k-1}(t) \right\}. \quad (\text{B.16})$$

In the case where  $k = 3$ , the first term is zero again, and in the diffusive limit this expression becomes

$$\frac{D}{Q} \left( \sum_{j=3}^Q \frac{1}{j} \right) \frac{\partial m}{\partial x} \Big|_{x=0}. \quad (\text{B.17})$$

For  $k > 3$ , it can be shown by induction that the general form for this equation after a total of  $s > Q + 1$  steps is

$$\frac{D\sqrt{\Delta t}}{Qh^2} \left\{ \left( \sum_{j=1}^{Q+k-s-2} \frac{1}{(k-j)^2} m_j(t) \right) \right. \\ \left. + \left( \frac{1}{(s-Q+1)^2} - \sum_{j=1}^{s-Q-1} \frac{k-3-j}{j^2} - \sum_{j=1}^Q \frac{1}{j} + (s-Q) \sum_{j=1}^{k-1} \frac{1}{j^2} \right) m_{Q+k-s-1}(t) \right. \\ \left. + \left( \sum_{j=1}^{s-Q} \frac{s-Q+1-j}{j^2} + \sum_{j=1}^Q \frac{1}{j} - (s-Q+1) \sum_{j=1}^{k-1} \frac{1}{j^2} \right) m_{Q+k-s}(t) \right\}, \quad (\text{B.18})$$

plus some vanishing second derivative terms. It therefore follows that after  $s = Q + k - 2$  steps the remaining terms will be

$$\frac{D\sqrt{\Delta t}}{Qh^2} \left\{ \left( \frac{1}{(k-1)^2} - \sum_{j=1}^{k-3} \frac{k-2-j}{j^2} - \sum_{j=1}^Q \frac{1}{j} + (k-2) \sum_{j=1}^{k-1} \frac{1}{j^2} \right) m_1(t) \right. \\ \left. + \left( \sum_{j=1}^{k-2} \frac{k-1-j}{j^2} + \sum_{j=1}^Q \frac{1}{j} - (k-1) \sum_{j=1}^{k-1} \frac{1}{j^2} \right) m_2(t) \right\}, \quad (\text{B.19})$$

which can be consolidated in the diffusive limit to yield

$$\frac{D}{Q} \left( \sum_{j=k}^Q \frac{1}{j} \right) \frac{m_2(t) - m_1(t)}{h} = \frac{D}{Q} \left( \sum_{j=k}^Q \frac{1}{j} \right) \frac{\partial u}{\partial x} \Big|_{x=0}. \quad (\text{B.20})$$

## Appendix C. Proof by induction: adsorption terms

We wish to evaluate

$$\frac{D\sqrt{\Delta t}}{Qh} \sum_{j=1}^{Q-k+1} \left[ \frac{P_{j+k-1,Q}}{(j+k-1)^2} m_j(t) \right]. \quad (\text{C.1})$$

We separate terms out into second derivatives as before, until the only terms which will not vanish in the diffusive limit are  $m_1$  and  $m_2$ ,

$$\begin{aligned} & \frac{D\sqrt{\Delta t}}{Qh} \left\{ \left( \frac{P_{k,Q}}{k^2} - \sum_{j=k+2}^Q \left[ \frac{(j-1-k)P_{j,Q}}{j^2} \right] \right) m_1(t) + \sum_{j=k+1}^Q \left[ \frac{(j-k)P_{j,Q}}{j^2} \right] m_2(t) \right. \\ & \left. + \left( \sum_{j=3}^{Q-k+1} \left[ \left( \sum_{i=j}^{Q-k+1} \frac{(i+1-j)P_{i+k-1,Q}}{i^2} \right) \frac{m_{j-2}(t) - 2m_{j-1}(t) + m_j(t)}{h^2} \right] \right) \right\}. \end{aligned} \quad (\text{C.2})$$

As our final step, we separate these terms into an expression in terms of  $m_1(t)$  alone, and a first derivative term,

$$\begin{aligned} & \frac{D\sqrt{\Delta t}}{Qh} \left\{ \left( \sum_{j=k}^Q \left[ \frac{P_{j,Q}}{j^2} \right] \right) m_1(t) \right. \\ & + \sum_{j=k+1}^Q \left[ \frac{(j-k)P_{j,Q}}{j^2} \right] h \left( \frac{m_2(t) - m_1(t)}{h} \right) \\ & \left. + \left( \sum_{j=3}^{Q-k+1} \left[ \left( \sum_{i=j}^{Q-k+1} \frac{(i+1-j)P_{i+k-1,Q}}{i^2} \right) \frac{m_{j-2}(t) - 2m_{j-1}(t) + m_j(t)}{h^2} \right] \right) \right\}. \end{aligned} \quad (\text{C.3})$$

The extra value of  $h$  means that first derivative terms also vanish in the diffusive limit, so taking that limit this expression will tend to

$$\frac{D\sqrt{\Delta t}}{Qh} \left( \sum_{j=k}^Q \left[ \frac{P_{j,Q}}{j^2} \right] \right) u(0, t), \quad (\text{C.4})$$

as stated in the main text.

## References

- [1] B. Bénazéraf, P. Francois, R. E. Baker, N. Denans, C. D. Little, and O. Pourquié. A random cell motility gradient downstream of FGF controls elongation of an amniote embryo. *Nature*, 466:248–252, 2010.
- [2] R. N. Thompson, C. A. Yates, and R. E. Baker. Modelling cell migration and adhesion during development. *Bull. Math. Biol.*, 74:2793–809, 2012.
- [3] M. J. Simpson, K. K. Treloar, B. J. Binder, P. Haridas, K. J. Manton, D. I. Leavesley, D. L. S. McElwain, and R. E. Baker. Quantifying the roles of cell motility and cell proliferation in a circular barrier assay. *J. Roy. Soc. Interface.*, 10:20130007, 2013.
- [4] H. G. Othmer, S. R. Dunbar, and W. Alt. Models of dispersal in biological systems. *J. Math. Biol.*, 26:263–298, 1988.

- [5] S. Engblom, L. Ferm, A. Hellander, and P. Lötstedt. Simulation of stochastic reaction-diffusion processes on unstructured meshes. *SIAM J. Sci. Comput.*, 31:1774–1797, 2009.
- [6] S. Isaacson and C. Peskin. Incorporating diffusion in complex geometries into stochastic chemical kinetics simulations. *SIAM J. Sci. Comput.*, 28:47–74, 2006.
- [7] C. A. Yates and R. E. Baker. Importance of the voronoi domain partition for position-jump reaction-diffusion processes on nonuniform rectilinear lattices. *Phys. Rev. E*, 88:054701, 2013.
- [8] A. Okubo. *Diffusion and Ecological Problems, Mathematical Models*. Springer-Verlag, 1980.
- [9] F. J. R. Meysman, B. P. Boudreau, and J. J. Middelburg. Relations between local, nonlocal, discrete and continuous models of bioturbation. *J. Mar. Res.*, 61:391–410, 2003.
- [10] R. Erban and S. J. Chapman. Reactive boundary conditions for stochastic simulations of reaction-diffusion processes. *Phys. Biol.*, 4:16–28, 2007.
- [11] R. E. Baker, C. A. Yates, and R. Erban. From microscopic to macroscopic descriptions of cell migration on growing domains. *Bull. Math. Biol.*, 72:719–762, 2010.
- [12] K. Painter and T. Hillen. Volume-filling and quorum-sensing in models for chemosensitive movement. *Can. Appl. Math. Quart.*, 10:501–543, 2002.
- [13] M. Mourão, D. Kreitman, and S. Schnell. Unravelling the impact of obstacles in diffusion and kinetics of an enzyme catalysed reaction. *Phys. Chem. Chem. Phys.*, 16:4492, 2014.
- [14] Y. Cao and L. Petzold. Accuracy limitations and the measurement of errors in the stochastic simulation of chemically reacting systems. *J. Comput. Phys.*, 212:6–24, 2006.
- [15] D. T. Gillespie. Exact stochastic simulation of coupled chemical reactions. *J. Phys. Chem.*, 81:2340–2361, 1977.
- [16] C. A. Yates and G. Klingbeil. Recycling random numbers in the stochastic simulation algorithm. *J. Chem. Phys.*, 138:094103, 2013.
- [17] M. A. Gibson and J. Bruck. Efficient exact stochastic simulation of chemical systems with many species and many channels. *J. Phys. Chem. A*, 104:1876–1889, 2000.
- [18] K. W. Morton and D. F. Mayers. *Numerical Solution of Partial Differential Equations: An Introduction*. Cambridge University Press, New York, NY, USA, 2005.
- [19] S. Lampoudi, D. T. Gillespie, and L. R. Petzold. The multinomial simulation algorithm for discrete stochastic simulation of reaction-diffusion systems. *J. Chem. Phys.*, 130:094104, 2009.
- [20] B. Bayati, P. Chatelain, and P. Koumoutsakos. Adaptive mesh refinement for stochastic reaction–diffusion processes. *J. Comput. Phys.*, 230:13–26, 2011.
- [21] J. Elf and M. Ehrenberg. Spontaneous separation of bi-stable biochemical systems into spatial domains of opposite phases. *Syst. Biol.*, 1:230–236, 2004.
- [22] S. A. Isaacson. A convergent reaction-diffusion master equation. *J. Chem. Phys.*, 139:054101,

2013.